

QUANTUM STATISTICS OF LIGHT
INTERACTING WITH MATTER

A THESIS

SUBMITTED TO THE DEPARTMENT OF PHYSICS
AND THE INSTITUTE OF ENGINEERING AND SCIENCE
OF BILKENT UNIVERSITY
IN PARTIAL FULFILLMENT OF THE REQUIREMENTS
FOR THE DEGREE OF
DOCTOR OF PHILOSOPHY

by

Ü. E. Müstecaplıoğlu

August 1999

THESIS

QC

174.4

.M87

1999

QUANTUM STATISTICS OF LIGHT INTERACTING WITH MATTER

A THESIS

SUBMITTED TO THE DEPARTMENT OF PHYSICS
AND THE INSTITUTE OF ENGINEERING AND SCIENCE
OF BILKENT UNIVERSITY
IN PARTIAL FULFILLMENT OF THE REQUIREMENTS
FOR THE DEGREE OF
DOCTOR OF PHILOSOPHY

by

Ö.E. Müstecaplıođlu

August 1999

Özge Müstecaplıođlu

100
174.4
1887
1893

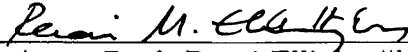
B C49037

I certify that I have read this thesis and that in my opinion it is fully adequate, in scope and in quality, as a dissertation for the degree of Doctor of Philosophy.



Prof. Alexander S. Shumovskiy (Supervisor)

I certify that I have read this thesis and that in my opinion it is fully adequate, in scope and in quality, as a dissertation for the degree of Doctor of Philosophy.



Assoc. Prof. Recai Ellialtıođlu

I certify that I have read this thesis and that in my opinion it is fully adequate, in scope and in quality, as a dissertation for the degree of Doctor of Philosophy.



Prof. Metin Gurses

I certify that I have read this thesis and that in my opinion it is fully adequate, in scope and in quality, as a dissertation for the degree of Doctor of Philosophy.


Asst. Prof. Zafer Gedik

I certify that I have read this thesis and that in my opinion it is fully adequate, in scope and in quality, as a dissertation for the degree of Doctor of Philosophy.


Prof. Tekin Derele

Approved for the Institute of Engineering and Science:


Prof. Mehmet Baray
Director of Institute of Engineering and Science

to Nihal

Abstract

QUANTUM STATISTICS OF LIGHT INTERACTING WITH MATTER

Ö.E. Müstecaplıođlu

M. S. in Physics

Supervisor: Prof. Alexander S. Shumovsky

August 1999

Studies on some systems in which light interacts with matter are performed from quantum statistical point of view. As a result of these studies a novel effect which can be utilized for detecting squeezed phonons is predicted; detection of non-classical states of Bose type excitations in solids and their classification by Raman correlation spectroscopy are discussed; a new approach to the polarization of light is developed.

Keywords: Quantum optics, Quantum statistics, squeezing, polarization, Raman scattering, non-classical excitations, multipole radiation

Özet

MADDE İLE ETKİLEŞEN IŞIĞIN KUVANTUM İSTATİSTİĞİ

Ö.E. Müstecaplıođlu

Fizik Yüksek Lisans

Tez Yöneticisi: Prof. Alexander S. Shumovsky

Ağustos 1999

Işık ve madde arasındaki etkileşimler çeşitli sistemler üzerinde kuvantum istatistiksel bakış açısıyla ele alındı. Bu çalışmaların neticesinde sıkıştırılmış fononların tesbitine olanak tanıyan yeni bir etki bulundu; Raman korelasyon spektroskopisi ile katılarda Bose türünden uyarılmaların klasik olmayan hallerinin sınıflandırılmasına ve tespitine imkan sağlayan yeni bir metot geliştirildi; ayrıca ışığın polarizasyonu hakkında yeni bir teori kuruldu.

Anahtar

sözcükler: Kuvantum optik, klasik olmayan uyarılmalar, Raman saçılması, sıkıştırılma, polarizasyon

Acknowledgement

I would like to express my deepest gratitude to Prof. Alexander S. Shumovsky for his supervision of my Ph.D. work in research, guidance, understanding, and friendship throughout the entire work.

I would like to thank Prof. S. John, and Prof. V. Rupasov of the Quantum Optics and Condensed Matter Research Group in University of Toronto for their hospitality and collaboration during my visit to University of Toronto, Prof. Barry Sanders of Macquarie University at Sydney, for fruitful and friendly discussions on the phase and polarization problems and their group theoretical studies, Prof. J. Eberly of Rochester Theory Center at University of Rochester, and Dr. L. Wang of NEC Research Institute at Princeton, New Jersey for their kind invitations for giving talks in their institutes, as well as useful discussions I enjoyed there.

I am indebted and grateful to my friends for their moral support as well as for discussions on many problems. Among my friends, I would like to give special thanks to Kaan Güven for everything. I also thank Mithat Ünsal for discussions.

Last but not least, my warmest thanks go to Mutluay and Müstecaplıoğlu families for their continuous trust, support and encouragement.

This thesis work is dedicated to my immortal beloved Nihal, as without her nothing would be possible...

This work is partially supported by a BDP grant through TUBITAK.

Contents

Abstract	i
Özet	i
Acknowledgement	i
Contents	i
List of Figures	iii
List of Tables	v
1 Introduction	1
1.1 Overview of Light-Matter Interaction	1
1.2 Why do we need statistical studies of that problem?	3
1.3 Quantum statistics or classical statistics?	4
1.4 Rabi oscillations in an exciton-polariton system	5
1.5 Non-classical states	6
1.6 Quantum Phase and Polarization	8
2 Squeezed Bosonic Excitations in Solids	10
2.1 Squeezed phonons	10
2.1.1 Model System	12
2.1.2 Realization of the effect	17
2.1.3 Summary	19

2.2	Examination of Non-Classical Quasi-particles with Raman Correlation Spectroscopy	20
2.2.1	Overview of the problem	20
2.2.2	Correlation of Stokes and anti-Stokes photons	23
2.2.3	Parametric Raman Model	26
2.2.4	Summary	31
3	Theory of Polarization	34
3.1	Vector Spherical Harmonics	34
3.2	Multipole Expansion of Electromagnetic Fields	38
3.2.1	General overview of evolution of radiation	38
3.2.2	Localized sources of radiation	40
3.2.3	Zones of radiation	40
3.2.4	Different zone behaviors illustrated:dipole radiation	41
3.3	Standard Classical Theory of Polarization	44
3.3.1	Poincaré Sphere	44
3.3.2	Operational approach to polarization	46
3.4	Standard Quantum Theory of Polarization	48
3.5	Systematic Approach to Multipole Radiation	52
3.5.1	Multipole fields at different zones of radiation	57
3.5.2	Separation of longitudinal part: electric, magnetic, and longitudinal vector spherical harmonics	58
3.5.3	Eigenfuctions of total angular momentum and polarization basis	60
3.6	Local Coherency Matrix and Stokes Operators	66
3.7	Polarization Matrix for Photons	69
3.8	Radiation along the z -Direction	73
3.9	Dipole radiation	74
3.9.1	Quantum fluctuations of the generalized Stokes parameters	75
3.9.2	Source-field communication in $E1$ -radiation	78
4	Conclusion	87

List of Figures

1.1	Basic scheme of light-matter interactions	1
1.2	Typical ways of light detection	4
1.3	Second order normalized correlation vs delay time	5
1.4	Experimental scheme for observing Rabi-oscillations in semiconductors	6
1.5	Regions in quadrature space	7
2.1	Squeezing of amplitude fluctuations of ionic oscillations illustrated	12
2.2	Level structure for indirect atomic transition	13
2.3	Phonon number distribution for squeezed thermal state	15
2.4	Distributions of chaotic phonons and coherent photons	16
2.5	Rabi oscillations of the cavity photons. Upper, and lower graphs correspond to thermal phonons at $300K$, squeezed thermal phonons with $r = 1$ at $10K$ respectively. Upper graph is shifted by 0.25 for better demonstration.	18
2.6	Band structure of <i>GaAs/AlAs</i> superlattice is shown with Type-I and Type-II transitions. $\Gamma - X$ transition is not shown, but it is also possible.	19
2.7	Phonon degree of coherence $G^{(2)}$ versus temperature for typical parameters of an ionic crystal: $\Omega = 200K$, $g = 25K$	23
3.1	Evolution of radiation, different spatial behaviors at different zones (stages) are illustrated.	39
3.2	Change of direction of electric field as radiation propagates	43
3.3	Poincaré sphere representation of transversal polarization states .	45

3.4	Variance of normalized S_1 compared with Pegg-Barnett approach. Lower curve is of the Pegg-Barnett cosine, the upper is of the C_R operator. Both curves are drawn for $\delta = 0$ and $I_+ = 0.275$	78
3.5	Evolution of the variance of the field cosine operator as a function of scaled time $t_s = gt/(2\pi(\bar{n}_- + \bar{n}_+)^{1/2})$ for $\bar{n}_\pm = 25$ and $g = 1$. Graphs from up to down correspond to the relative phases $\delta = 0, 45, 75, 90$ in degrees , respectively.	86

Chapter 1

Introduction

1.1 Overview of Light-Matter Interaction

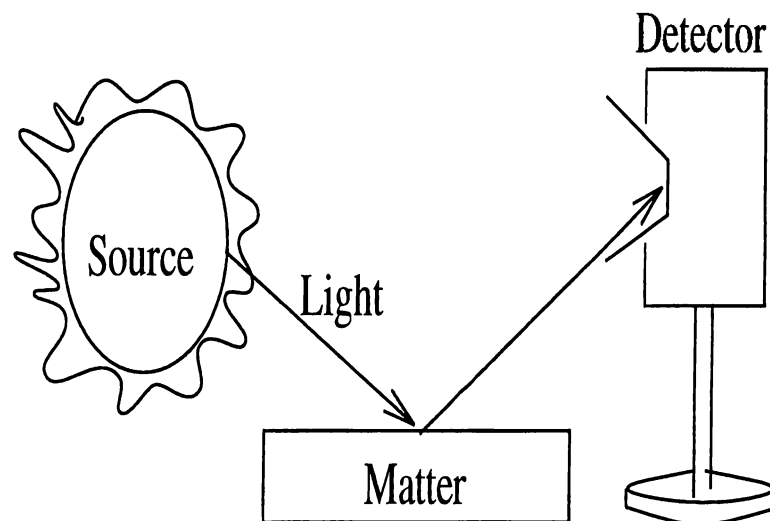


Figure 1.1: Basic scheme of light-matter interactions

The dream of enhancing sensitivity in a spectroscopic measurement beyond the usual quantum limit set by the vacuum fluctuations has come true after the realization of non-classical states of light. Particularly using squeezed light for such a purpose provides exciting and rich possibilities. It is possible to say that where ordinary light remains blind, squeezed light may be sharp eyed.

For example the Doppler-free resonances in atomic cesium is observed with a sensitivity higher than the vacuum-limit by using a frequency-tunable squeezed light.¹ No doubt in a spectroscopic measurement light interacts with matter under examination, and transfers us the information we are after. It is therefore necessary to have a thorough study of this interaction in order to understand what kind of extra information can be extracted from the matter. Huge number of studies in the area shows that the field correlation functions involve information on the source correlation functions. Hence, the examination of the problem of light-matter interaction from a complete quantum statistical point of view is essential. Let us also note that the potential applications of non-classical light is not limited to spectroscopy. There are other technological fields, especially optical communications, demanding high degree of noise reduction. High sensitive interferometric methods are also required to detect gravitational waves.

It is possible to classify the studies on the problem of interaction of light with matter under three main groups as shown in Fig.1.1. First one focuses on the generation of light by the matter, second one examines the effects of light on the creation and the statistics of quasiparticles within the matter, and the last one treats light as the carrier of information about the matter. It must be emphasized that in reality, those subjects are interwovenly mixed and this classification scheme does not mean the problem is separable, rather it only reflects the hubs of attentions of the scientists working in the area. Clearly, the categories are so broad that one expects a lot of sub-branches related to them. Therefore, it is beyond a single thesis to cover all of them. In Ref.² we have examined the problem of Rabi oscillations in an exciton-polariton system prepared in a high quality microcavity. We have found there some optimum conditions for the observation of these oscillations. Besides explicit relations between the cavity damping rate and the form of the oscillations were established. An expression for the renormalized Rabi frequency was also derived. The agreement of our results with the experimental ones can be considered as a good example for demonstrating the success of applying atomic quantum optical models to solid state systems under special conditions.³ Since that analysis might be associated

with the first group, we have turned our investigations towards the latter two. We have picked up an important and interesting problem for each group to analyze. The problem of generation and detection of squeezed phonons and the problem of polarization of electromagnetic radiation were examined for the second and third groups, respectively.

1.2 Why do we need statistical studies of that problem?

We know that all detecting devices absorbs light, and the basic mechanism of detection is just the light absorption. As a result, a photocurrent is created in photodetectors, or light absorbed by phosphorus atoms and we see an illumination on the screen. Even our eyes absorbs light and send signals to the brain and vision is recorded. Electric field can be written in terms of positive and negative frequency components. Positive frequency component is associated with absorption process while the negative frequency component is associated with the generation of light process.

$$E = E^+ + E^-, \quad E^\pm \propto e^{\mp i\omega t}. \quad (1.1)$$

During the generation or interaction of light with environment, light gathers parameters related to the interaction and generation. These parameters are subject to statistical variability. In quantum theory, there is also an unavoidable background shot noise, associated with the quantum fluctuations in accordance with the uncertainty principle. In measurements, such fluctuations and statistical variabilities are usually tried to be minimized by repeated measurements. This brings the concept of ensemble averaging.

We can summarize some typical measurement schemes shown in Fig.1.2, and write down what we observe in each of them.

- Screen measures $\langle E^-(1)E^+(2) \rangle$;
- Single photodetector measures $\langle E^-(1)E^+(1) \rangle$

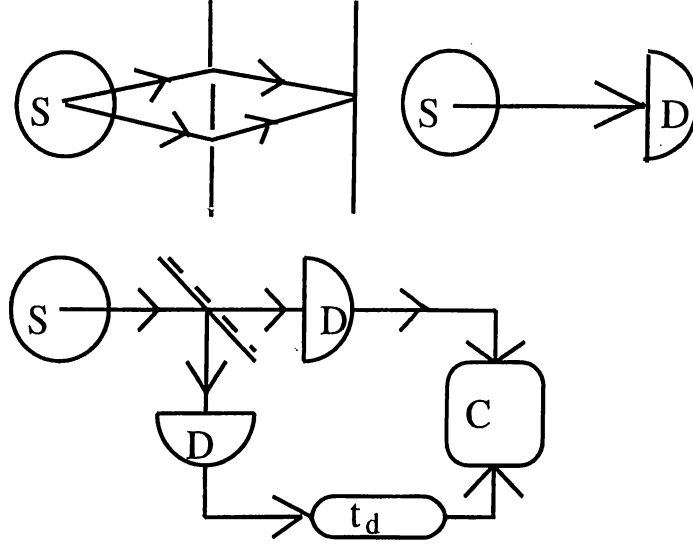


Figure 1.2: Typical ways of light detection

- Correlator (multiplier) measures $\langle E^-(0)E^-(t_d)E^+(t_d)E^+(0) \rangle$

As we see, it is convenient to define n-th order correlation function :

$$G^{(n)}(x_1, \dots, x_n, y_n, \dots, y_1) = \langle E^-(x_1) \dots E^-(x_n) E^+(y_n) \dots E^+(y_1) \rangle, \quad (1.2)$$

since in measurements, the observable parameters can be expressed in terms of such correlation functions.

1.3 Quantum statistics or classical statistics?

It is also convenient to define a normalized correlation function

$$g^{(2)}(t_d) = \frac{G^{(2)}(t_d)}{|G^{(1)}(0)|^2} \quad (1.3)$$

Experimental studies of that correlation function yield an important effect, namely anti-bunching property of light in resonance fluorescence. Light from thermal sources (stars) is called as incoherent light. In that case, it is found that $g^{(2)} > 1$. This shows probability of detecting two photon in a short time interval of detection is higher than detecting photons separately. This preference

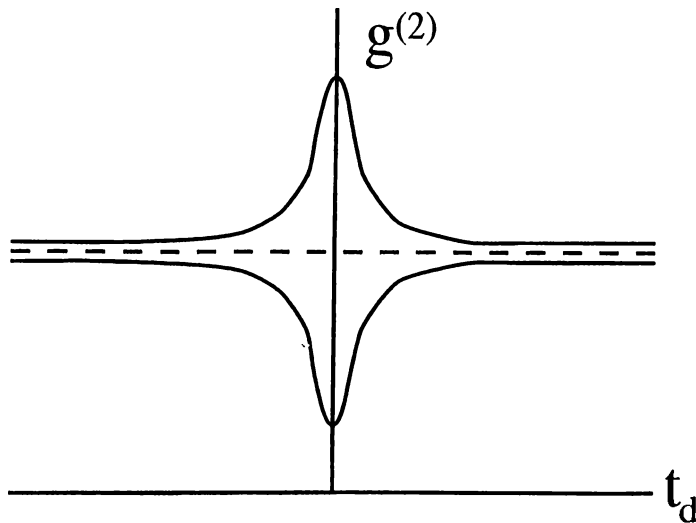


Figure 1.3: Second order normalized correlation vs delay time

of becoming together can be considered as typical for bosons. This effect can be explained in classical physics. On the other hand, light from resonance fluorescence show anti-bunching effect, with $g^{(2)} < 1$. These are shown in Fig.1.3. As an important conclusion we see that quantum effects can be best found in high order interference experiments.

1.4 Rabi oscillations in an exciton-polariton system

We review this subject for completeness and as an example of light generation process. $GaAs/Al_xGa_{1-x}As$ short-period superlattice is placed in a cavity of distributed Bragg reflectors (DBR), and pumped by a Ti-Sapphire laser. Emitted radiation from the cavity is focused on a BBO (Beta-Barium Oxide) crystal and time-delay spectroscopic analysis is performed to detect Rabi beats. Experimental set-up and procedure is summarized in Fig.1.4. We considered an exciton-polariton model to explain the obtained experimental data. Output light can be generated with desired properties just by controlling external

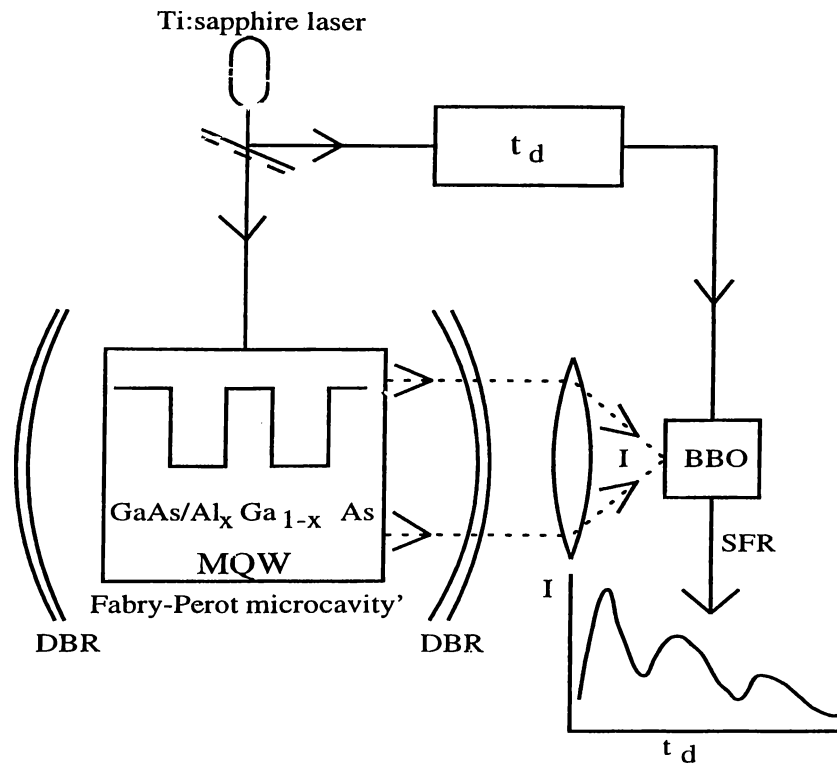


Figure 1.4: Experimental scheme for observing Rabi-oscillations in semiconductors

parameters. Several conclusions are

- pump frequency, excitonic gap \rightarrow amplitude, number of beats in output
- The cavity quality \rightarrow qualitatively different damping regimes.
- Strong pulses as pump \rightarrow coherent output, coherent polaritons

This study is a good example to demonstrate success of (atomic) quantum optical models in solid state systems.

1.5 Non-classical states

Let us review also some important states of light. For classification of states

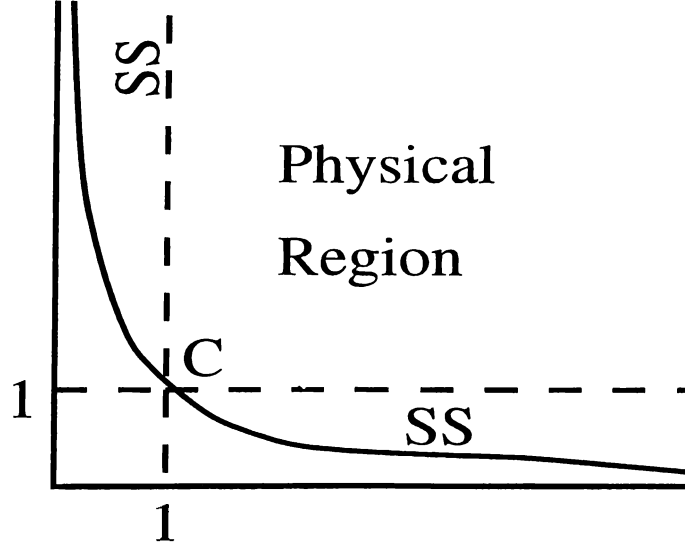


Figure 1.5: Regions in quadrature space

of light it is convenient to define quadratures as the real and imaginary part of the annihilation operator,

$$E^{(+)} \sim a, \quad a = \frac{X_1 + iX_2}{2}, \quad (1.4)$$

They have the uncertainty relation,

$$\Delta X_1 \Delta X_2 \geq 1 \quad (1.5)$$

Uncertainty relation is drawn as Fig.1.5. Coherent and squeezed light is most common states of light. Their properties are summarized below. They are also classified on the Fig.1.5.

- Coherent states

$$a |\alpha\rangle = \alpha |\alpha\rangle, \quad \Delta X_{1,2} = 1, \quad (1.6)$$

$$|\alpha\rangle = \exp(\alpha a^\dagger - h.c.) |0\rangle, \quad H_{int} = \alpha a^\dagger + h.c. \quad (1.7)$$

- closest to classical descriptions
- indefinite number of photons, well defined phase
- nonorthogonal, normalized, overcomplete

- Squeezed States

$$\Delta X_1 > 1 > \Delta X_2, \quad (1.8)$$

$$|z\rangle = \exp(1/2z^*a^2 - h.c.) |0\rangle, \quad H_{int} = z^*a^2 + h.c. \quad (1.9)$$

1.6 Quantum Phase and Polarization

Because of the close connection of phase and polarization problem, we review the quantum phase problem of light here. Since the early years of quantum mechanics the introduction of amplitude and phase operators especially for the electromagnetic field is under debate. The first approach to the problem was based on the direct factorization of ladder operators.¹⁷ Unfortunately, the phase operator constructed by this way yields unphysical fluctuations which are greater than 2π . Besides it contradicts the assumption of Hermiticity which is the natural expectation for an operator claiming to represent phase as a physical observable. After noticing the direct approach to the problem is closed, alternative routes to overcome the problem are considered. In order to solve the trouble with Hermiticity, Hermitian and periodic cosine and sine operators were constructed.^{18,19} However they carry an unpleasant property of non-commutativity which results in the impossibility of describing a single phase angle by them. Later, lack of a well-defined Hermitian phase operator is connected to the boundedness of the spectrum of the number operator which should be conjugate to the phase operator.²⁰ Following that, many proposals allowing the negative part of the spectrum have appeared.²¹ Due to the presence of non-physical states, they are not widely-accepted. In a more recent proposal a truncated Hilbert space is used for the description of quantum states of the electromagnetic field modes.²² According to that prescription the correct expectation values are evaluated by enhancement of the truncated space to the standard infinite dimensional Hilbert space by taking the limit over the space dimension variable after the expectation values are evaluated first in the finite space. Even though this is the most widely accepted quantum phase theory, it still

suffers some serious problems like changing the algebraic properties of photons. Since photons are governed by the Weyl-Heisenberg algebra, the truncation of the Hilbert space causes a serious change in the commutation relations defining the algebra. In that sense the limiting procedure involves unclear and unphysical points. Other than those first-principle attempts there are also theories based upon quantum estimation theory which give similar results with the finite Hilbert space method, quasiprobability distributions which might yield negative phase distributions in some cases, and optical homodyne tomography. Without an explicitly constructed phase operator some information on the phase properties of the field can still be gained within these approaches (For a review see²³ and references therein). The operational approach to the quantum phase has been presented recently²⁴ where the phase is defined in terms of the measurement schemes. In that point of view there cannot be a unique phase operator due to the dependence on experimental set up. However it has been shown that the phase distribution of the operational approach is a known quasi probability distribution and there should be a unique phase operator associated to the experimental set-up considered in the operational approach. Another contribution to the problem has been made by considering the Stokes parameters used for description of the polarization properties of the classical radiation. Quantization of these parameters lead to the so called Stokes operators which can be decomposed in polar form to describe the phase properties of radiation quantum mechanically.²⁵ However the lack of unique phase angle still persist in that approach, too. As one can appreciate there are so many ingenious attempts and proposals to solve the problem of quantum phase. Even though they have some usefulness in certain areas and can solve some parts of the problem there is no complete answer to that old question.

Chapter 2

Squeezed Bosonic Excitations in Solids

2.1 Squeezed phonons

It has been known for a long time that science of acoustics bears a lot of similarities to the science of optics so that it is also called as the phonon optics (see Ref.^{4,8} and references therein). While these analogies are based on classical effects, quite recently some scientists start to ponder upon the possibilities to observe nonclassical effects of photon optics in the phonon optics. Much of these effects, like photon antibunching, squeezing and non-classical photon distributions, arise as a result of the Bose-Einstein statistics of the photons. Since there are a number of quasi-particles which obey the same statistics in solids, the expectation to find similar effects in solid state media should not be a poor one. Among these particles, the phonons have already been known to contribute highly non-classical effects where the consideration of quantum optical analogies proved to be helpful. For example, the broad Raman line shape anomaly in the Raman spectra of some high- T_c compounds such as La_2CuO_4 and $YBa_2Cu_3O_{6.2}$ at around 3230 and 3080cm^{-1} respectively, is associated with the quantum fluctuations in the atomic positions.⁵ There are also attempts to explain some other properties of high- T_c materials including their isotope anomalies by introducing anharmonic

phonon correlations to the conventional Frölich interactions.⁶ Older examples in which the phonon correlations play an important role are the Peierls transition and the Jahn-Teller effect. It is known in quantum optics that anharmonic correlations may result in the decrease of fluctuations of a dynamic variable below the quantum limit at the cost of increasing fluctuations of its quantum conjugate variable. Such phenomena is called as squeezing. Thus, nowadays the above mentioned effects are usually described in terms of squeezed phonons. While the squeezing of localized phonons was examined a while ago,⁷ the question of how to generate phonon squeezed states in solids was tried to be answered only recently by some proposals including a three-phonon parametric amplification process,⁴ phonon-photon coupling in polaritons,^{4,8} and second order Raman scattering process⁴ which was very recently demonstrated experimentally.⁹ The mechanism behind the generating squeezed phonons is based upon application of ultra short pulses on a second order Raman active crystal. When no light is acted upon the crystal, phonons are associated with ionic oscillations. Fluctuations do occur in the oscillations, which we can imagine as random displacement of ions. Some ions would be displaced longer than necessary, and some would be displaced less than necessary for noiseless phonon states. On the other hand, it can be shown that ultra short pulses ‘kick’ ions regularly so that they apply a force proportional to displacement. In other words, ions displaced further than necessary would feel a force stronger than those ions with less displaced. Thus, the ultra short pulses have a regularization effect which put the ions into an order. In Fig.2.1, we illustrated this phenomenon.

At the same time, the problem of how to detect non-classical phonons was considered.¹⁰ Since the direct detection schemes via phonon counters¹¹ are almost impossible due to their low efficiency and wideband characteristics, alternative detection schemes based on reflectivity measurements⁴ and neutron scattering¹⁰ were discussed. Here, we introduce another indirect way of detecting the presence of squeezing in phonons. It is based on an effect which is the reduction of the revival time of Rabi oscillations of the intensity of photons interacting with squeezed phonons through an indirect radiative transition.¹² We also present

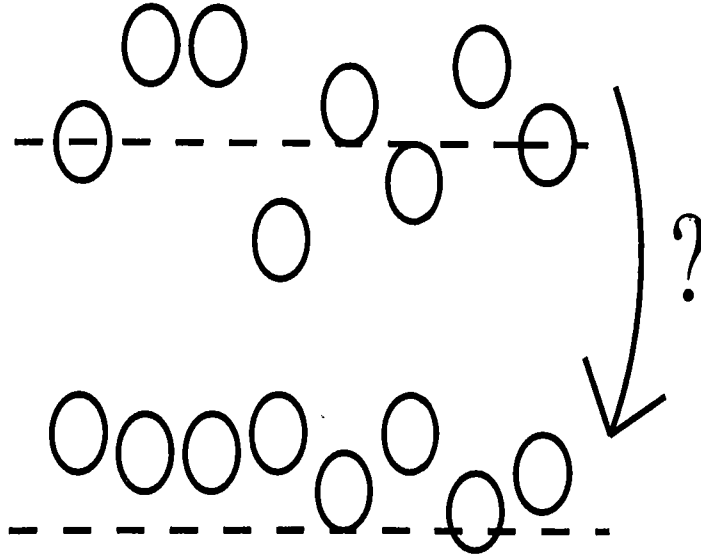


Figure 2.1: Squeezing of amplitude fluctuations of ionic oscillations illustrated some means of generating such interesting states.

2.1.1 Model System

Description of the indirect radiative transition in a simple way can be accomplished by modeling it with a generalized Jaynes-Cummings Hamiltonian with two boson transition. This model is examined in great detail for different problems of quantum optics.¹⁴ We suppose that the phonons belong to the longitudinal optical (LO) branch. The upper and lower atomic levels are denoted by ϵ_1 and ϵ_0 , respectively. Then, for the model illustrated in Fig.2.2, we write the Hamiltonian in units of \hbar as

$$H = \left(\Omega + \frac{\Delta}{2}\right)S_z + (\Omega + \epsilon)b^\dagger b + (\Omega - \epsilon)a^\dagger a + g(a^\dagger b^\dagger S_- + h.c.), \quad (2.1)$$

$$\Omega \equiv \frac{\omega_{LO} + \omega}{2}, \quad \epsilon \equiv \frac{\omega_{LO} - \omega}{2}, \quad \Delta \equiv (\epsilon_1 - \epsilon_0) - 2\Omega.$$

Here, ω_{LO} is the LO-phonon frequency, ω is the photon frequency, $S_{\pm,z}$ are the atomic projection operators, a, b are the photon and phonon operators, respectively. We have written this Hamiltonian in rotating wave approximation and ignored the intermediate levels and Stark shifts. Within the manifold

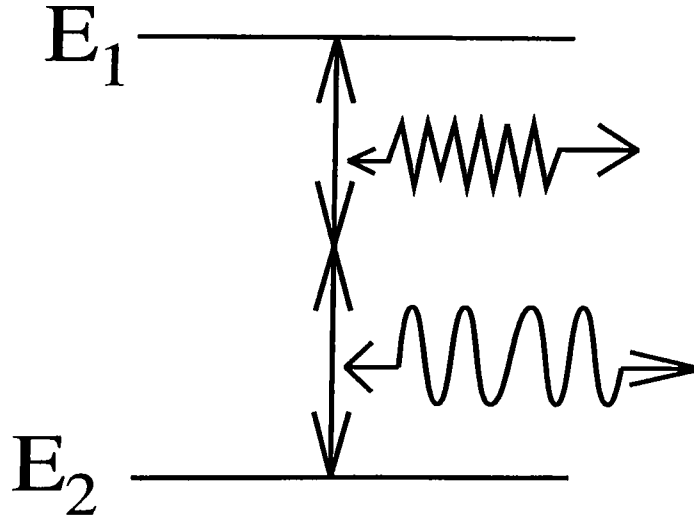


Figure 2.2: Level structure for indirect atomic transition

$\mathcal{M}(n, m)$ spanned by the bare state basis $\phi_1 = |1; n, m\rangle$, $\phi_0 = |0; n+1, m+1\rangle$ where n, m stand for photon and phonon numbers, respectively and first index labels the atomic states. Then Eq.2.1 becomes

$$H = \begin{pmatrix} E_0 + \frac{\Delta}{2} & \tilde{g} \\ \tilde{g} & E_0 - \frac{\Delta}{2} \end{pmatrix} \quad \text{where,} \quad (2.2)$$

$$E_0 \equiv \Omega(1+n+m) + \epsilon(m-n), \quad (2.3)$$

$$\tilde{g} \equiv g\sqrt{(n+1)(m+1)}. \quad (2.4)$$

Diagonalization of eq.2.2 is equivalent to an improper rotation of the bare state basis into the dressed state basis $\{\psi_+, \psi_-\}$ with the corresponding eigenenergies $E_{\pm} = E_0 \pm \Omega_R$, where the Rabi frequency Ω_R is defined as

$$\Omega_R \equiv \sqrt{\tilde{g}^2 + \frac{\Delta^2}{4}}, \quad (2.5)$$

$$\begin{pmatrix} \psi_+ \\ \psi_- \end{pmatrix} = \begin{pmatrix} c & s \\ s & -c \end{pmatrix} \begin{pmatrix} \phi_1 \\ \phi_0 \end{pmatrix}, \quad \text{with} \quad (2.6)$$

$$c = \sqrt{\frac{\Omega_R + \Delta/2}{2\Omega_R}}, \quad (2.7)$$

$$s = \sqrt{\frac{\Omega_R - \Delta/2}{2\Omega_R}}. \quad (2.8)$$

Then, we evaluate the propagator $U = e^{-iHt}$ as

$$U = \begin{pmatrix} c^2 e^{-iE_+ t} + s^2 e^{-iE_- t} & sc(e^{-iE_+ t} - e^{-iE_- t}) \\ sc(e^{-iE_+ t} - e^{-iE_- t}) & s^2 e^{-iE_+ t} + c^2 e^{-iE_- t} \end{pmatrix} \quad (2.9)$$

Since we deal with a field in a mixed state, we consider the density matrix and its time evolution which is determined by $\rho(t) = U(t)\rho(0)U^\dagger(t)$. Assuming the following initial preparation of the system,

$$\rho(0) = \sum_{n,m} \sum_{n',m'} F_{n,m} F_{n',m'}^* |1; n, m\rangle \langle 1; n', m'| \quad (2.10)$$

we find the reduced density matrix of the fields, given by the partial trace $P_{n,m}(t) \equiv \rho_{n,m;n,m}^F(t) = \sum_{k=0,1} \langle k; n, m | \rho(t) | k; n, m \rangle$, as

$$P_{n,m} = P_{n,m}(0) \left(1 - \frac{\tilde{g} \sin^2 \Omega_R t}{\Omega_R^2}\right) + P_{n-1,m-1}(0) \frac{g^2 n m \sin^2 \Omega_R (n-1, m-1) t}{\Omega_R^2 (n-1, m-1)}. \quad (2.11)$$

Thus, for the intensity of photons $I(t) \equiv \langle n(t) \rangle = \sum_{n,m} P_{n,m}(t) n$ we obtain,

$$I(t) = \langle n(0) \rangle + \sum_{n,m} P_{n,m}(0) \frac{\tilde{g}^2 \sin^2 \Omega_R t}{\Omega_R^2}. \quad (2.12)$$

For the initial distributions of the fields we choose $P_{n,m}(0) = P(n)\eta(m)$ such that $P(n) = \exp(-\bar{n})\bar{n}^n/n!$ is the Poisson distribution of coherent photons, and $\eta(m)$ is the number distribution of squeezed thermal phonons¹⁵ which is demonstrated in Fig.2.3, given by

$$\eta(m) = \frac{1}{1+\bar{m}} \sum_l \left(\frac{\bar{m}}{1+\bar{m}}\right)^l \begin{cases} 0, & \text{when } |l-m| \text{ is odd;} \\ \frac{l!m!}{(\cosh r)^{2l+1}} \left(\frac{1}{2} \tanh r\right)^{m-l} K(l,m), & \text{otherwise.} \end{cases} \quad (2.13)$$

Here, squeezing parameter $r \in \Re$, and

$$\bar{m} = \frac{1}{e^{\omega_{LO}/T} - 1}, \quad K(l,m) = \left| \sum_k \frac{(-)^k (2^{-1} \sinh r)^{2k}}{k!(l-2k)![k+(m-k)/2]} \right|^2.$$

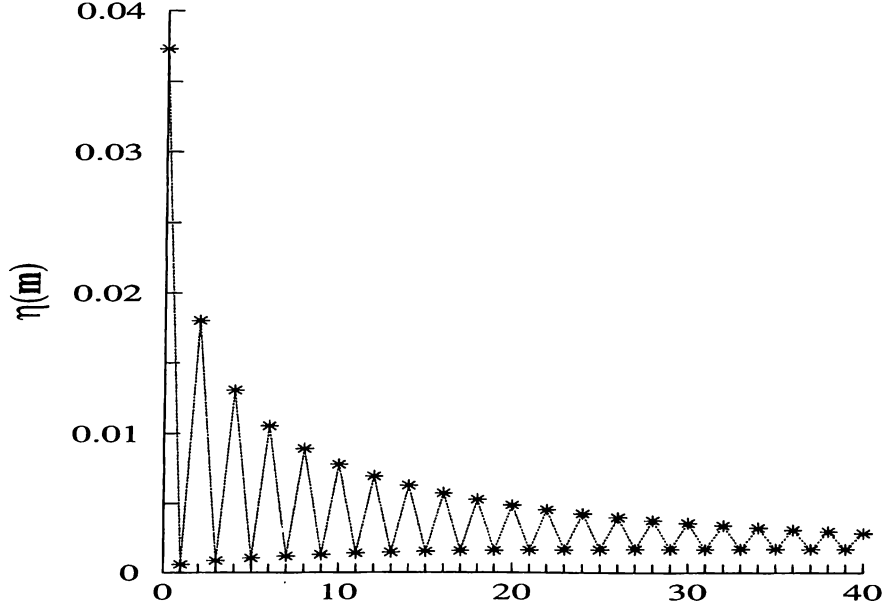


Figure 2.3: Phonon number distribution for squeezed thermal state

In Fig.2.4, the chaotic thermal distribution and Poisson distribution are shown. As one can see, while phonons with coherent distribution can be distinguished more clearly from chaotic and squeezed ones, the distinction between chaotic and squeezed ones in qualitative terms is harder. In fact, the only distinction is the oscillatory character of squeezed distribution, and this is not easy to observe directly, since tomographic direct construction methods is hard to associate with phonons. Here, the effect which we will describe will be an indirect way to find an effect arising from these oscillations. Since the Poisson distribution is peaked around \bar{n} , we can apply the saddle point analysis³⁷ in Eq.2.12 to calculate the summation over index n . The result is

$$I = \bar{n} + \frac{1}{2} - \frac{1}{2} \sum_{k,m=0}^{\infty} h_k \eta(m) e^{-4(\tau - \tau_{km})^2 / \Delta \tau_{km}^2} \cos \phi_{km} \quad (2.14)$$

where,

$$h_k = (1 + k^2 \pi^2)^{-1/4}, \quad (2.15)$$

$$\tau = \frac{gt}{2\pi\sqrt{\bar{n}}}, \quad (2.16)$$

$$\tau_{km} = \frac{k}{\sqrt{m+1}}, \quad (2.17)$$

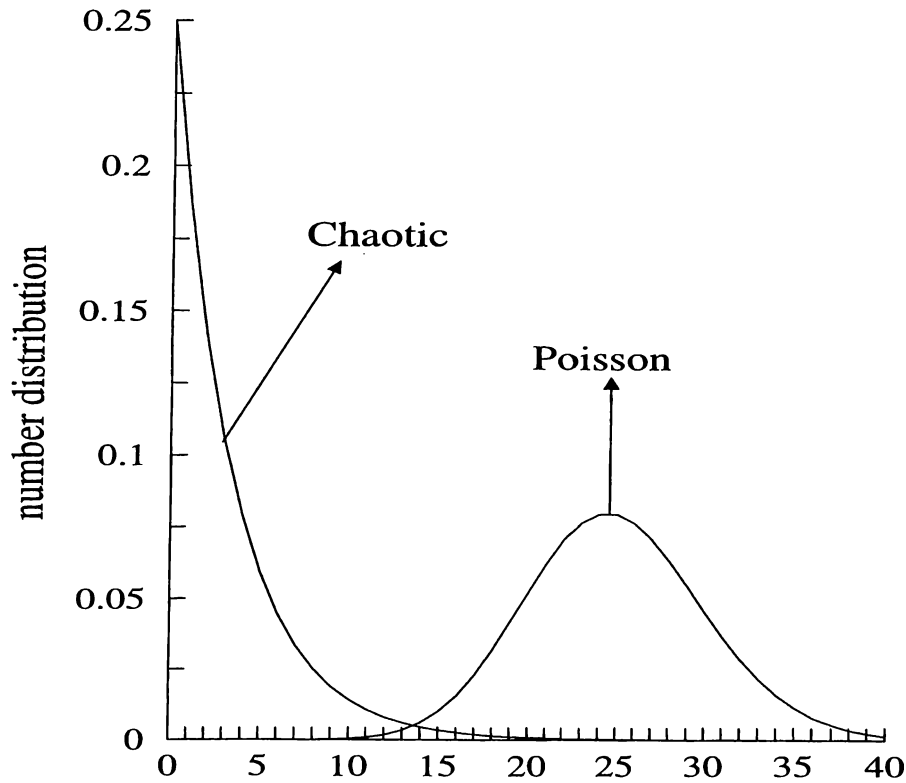


Figure 2.4: Distribution of particles and coherent photons

$$\epsilon_{km} = \pi(\tau\sqrt{m+1} - k), \quad (2.18)$$

$$\phi_{km} = \bar{n}(2k\pi + 4\epsilon_{km} + k\pi 2h_k^4 \epsilon_{km}^2) - \frac{1}{2} \tan^{-1}(k\pi) + 2h_k^4 \epsilon_{km}, \quad (2.19)$$

$$\Delta\tau_{km} = 2\sqrt{\frac{1 + k^2\pi^2}{2\bar{n}(m+1)\pi^2}}. \quad (2.20)$$

We now clearly see that the resulting intensity consists of interfering Gaussians which are revivals of the intensity. They are peaked at revival times τ_{km} , with widths $\Delta\tau_{km}$. Their heights depend on phonon number distribution. The distribution described in Eq.2.13 shows pairwise oscillations. The oscillations are much more pronounced at low temperatures and higher r . For $r = 0$, $\eta(m)$ reduces the thermal distribution which is monotonically decreasing with m . The intensity we found in Eq.2.14 is governed by the first few terms since the amplitude, $h_k\eta(m)$, of the Gaussian envelopes is a decreasing function of indices k, m . At 10K, the dominating terms would be $(k = 0, m = 0), (k = 1, m = 0, 1, 2)$. Among them the term with $m = 1$ may be negligibly small

if the amplitude $\eta(1)$ is small compared to $\eta(0)$ and $\eta(2)$ as in the case of squeezed thermal distribution. However, it surely dominates the term with $m = 2$ for thermal distribution. Since, m also determines the peak positions of the Gaussians through τ_{km} , we have a qualitative way of distinguishing both distributions from each other by the absence of the revivals associated with odd m integers in the presence of squeezing. This is illustrated in Fig.2.5. Instead of the approximate result, Eq.2.14 we have carried out exact numerical summation to get those figures. However, even using the first four terms of eq.2.14 we can obtain figures with excellent resemblance to those. We used 20meV for ω_{LO} which is typical for *GaAs*. Therefore, the LO-phonon density is almost zero, and the phonon number distribution is close to that of vacuum squeezed state in which probability of having odd number of phonons vanishes for any $r > 0$. Thus, even in the case of weak squeezing, the effect can be a valuable tool. Note that, for any two integers k, m satisfying $m = 3k^2 - 1$, the corresponding Gaussian is peaked at τ_{km} . Therefore the best place to estimate the amount of squeezing is the peak at $\tau = 0$ where $k, m = 0$, since only one Gaussian can be placed there. The corresponding amplitude from which r can be found is $\eta(0) = 1/\sqrt{(1 + 2\bar{m}) \cosh^2 r + \bar{m}^2}$. Finally, we note that, since the squeezed thermal distribution has higher mean value and variance, we may get hints on the presence of squeezing by the increasing number of revivals before $\tau = 1$ with narrower widths through $\Delta\tau_{km}$, even for the cases in which the oscillations in the phonon number distributions are weak.

2.1.2 Realization of the effect

To be able to realize the above mentioned effect, we need first of all a solid state material in which strong radiative indirect transitions are possible. Moreover, it must be prepared to have squeezed phonons. Then it should be enclosed in a high quality cavity, since we considered only one cavity mode and ignored the cavity damping. A promising candidate of such a material is provided by *GaAs/AlAs* short period superlattices,³⁸ band structure of which is shown in Fig.2.6.

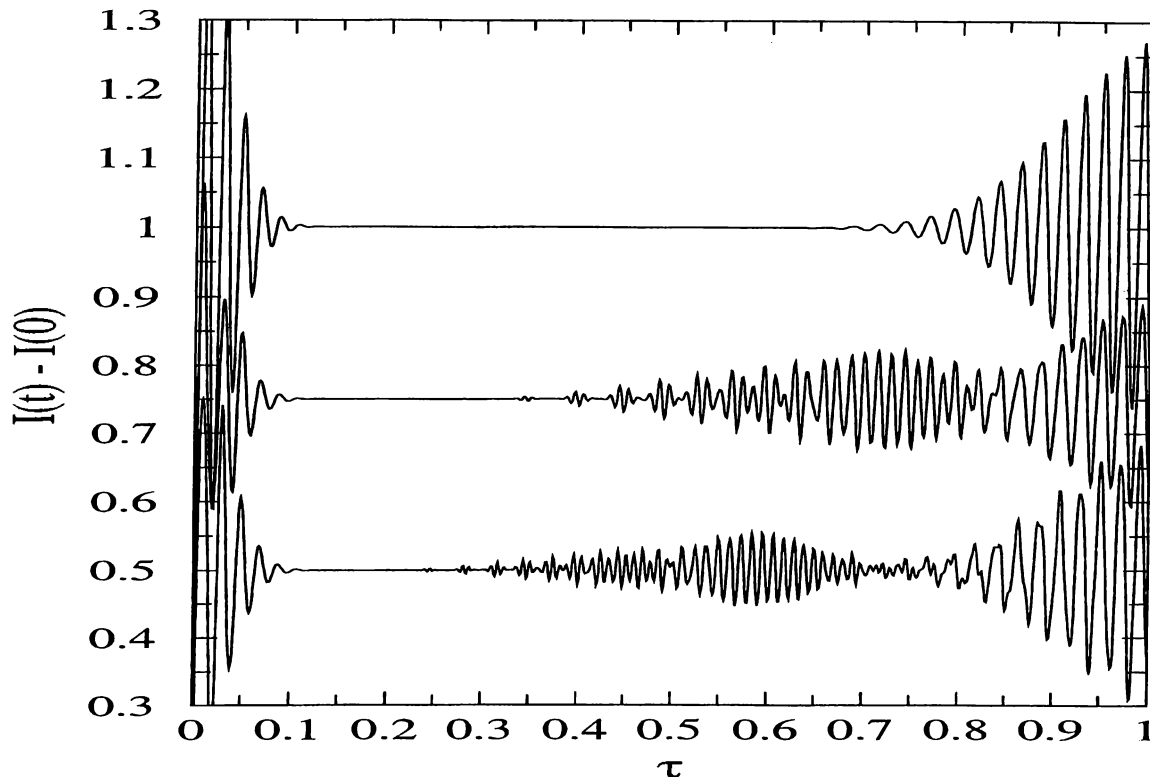


Figure 2.5: Rabi oscillations of the cavity photons. Upper, and lower graphs correspond to thermal phonons at $300K$, squeezed thermal phonons with $r = 1$ at $10K$ respectively. Upper graph is shifted by 0.25 for better demonstration.

There, the direct, type-I, transition is accomplished by single photon emission-absorption, while the indirect, type-II, transition is occurred as an LO-phonon assisted single photon emission-absorption. Depending on the quantum well thickness, the $\Gamma-X$ transition is also possible via LO-phonon absorption, emission and interface scattering. We shall consider thick enough wells to eliminate the interface scattering and this leaves us only Frölich interaction of electrons with LO-phonons. At low temperatures ($T \approx 8K$), with high excitation density (laser power $\approx 12mW \rightarrow$ excitation density $\approx 3 \times 10^{11} cm^{-2}$) and with excitation energy a little higher than the type-I transition resonance (laser energy $\approx 1.96eV$), the dominant transition becomes type-I because of the band-filling effects at X . Thus we have effectively a Λ -shaped three level system. Due to the high excitation densities the electron-subsystem is in the quasi equilibrium regime; besides, the high density coherent laser field can also be treated classically. Therefore, treating

only the phonons with operators, we get an effective interaction Hamiltonian as $H_{eff} = \sum_k g_k b^k + h.c.$, where g_k 's depends on carrier concentrations and Frölich interaction strengths. Among possible multiphonon interactions, we can take the quadratic one as the dominant, if the $\Gamma - X$ separation is about twice the LO-phonon energy ($w_{LO} \approx 10 - 30 meV, GaAs$). Such a Hamiltonian generates squeezed thermal phonons, if we suppose the phonon sub-system is in thermal equilibrium before the action of the laser field. Since the lifetime of the electrons in X states is much higher than the type-I recombination (at $8K, t_X = 0.7 \mu s, t_{type-I} = 200 ps$), we conclude that the system is prepared in the way described by Eq.2.10 with squeezed thermal phonons. Then, by increasing the laser energy (> 2.014), decreasing the laser power ($< 2.4 mW$), and providing a weak probe coherent light to observe the changes in collapse and revivals of its intensity we should be able to observe this effect.

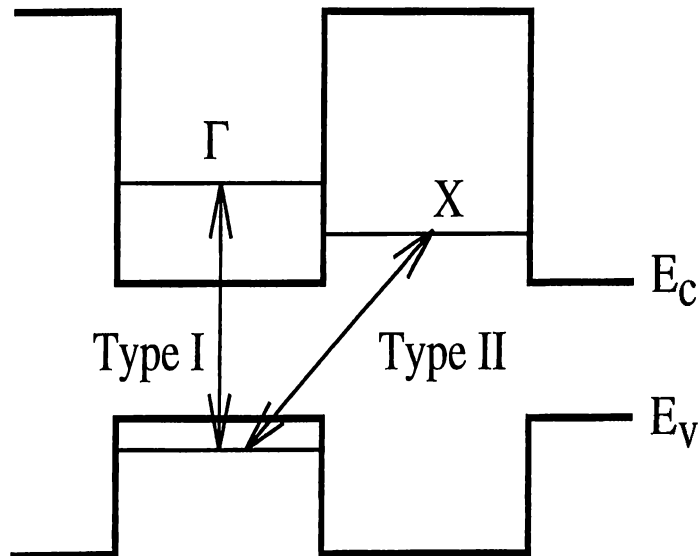


Figure 2.6: Band structure of $GaAs/AlAs$ superlattice is shown with Type-I and Type-II transitions. $\Gamma - X$ transition is not shown, but it is also possible.

2.1.3 Summary

Detection of squeezed phonons through an indirect radiative transition is discussed. It is shown that lack of certain revivals at low temperatures can

be considered as the signature of squeezing. At high temperatures, the effect can still be observed for high squeezing. In any case, squeezing manifest itself also with narrower and more revivals in the standard collapse region ($\tau < 1$). It is possible to estimate the squeezing parameter from the amplitude of the revival at $\tau = 1$. *GaAs/AlAs* superlattice structures are suggested for the realization of the proposed scheme considering their analogy to the three level systems discussed in quantum optics.

2.2 Examination of Non-Classical Quasi-particles with Raman Correlation Spectroscopy

We have seen that squeezed states of phonons can have useful application in optical communications as offering a way to reduce and control revival times. Higher order squeezing can offer even more reduction in the revival times. Interaction of such phonons with other quasi-particles as well as electrons would also be interesting for other electrical and optical effects related with solids. In fact, squeezed states, or in general non-classical states of other quasi-particles can also be found. In some case, like polaritons, natural formation of such two particle bound states are also more readily squeezed or non-classical. Therefore, it is an important study to examine the problem how to detect and classify such non-classical quasi-particles. Below, we present a way to do this using Raman correlation spectroscopy.¹³

2.2.1 Overview of the problem

The concept of squeezed state has been established in the language of physics mainly by the developments in quantum optics. On the other hand, basic requirement of finding a system in a squeezed state is to have bosons as the constituents of the system interacting in a pairwise manner and that might be

fulfilled not only in optical systems but in some other Bose-type systems as well. The introduction of squeezed states in optics³⁹ was based on the previous consideration of superfluidity⁴⁰ in liquid He^4 (also see⁴¹). While squeezing of quantum fluctuations is the most well-known aspect of squeezed states, rich variety of effects might be expected due to their interesting statistical properties even at thermal equilibrium. Certain effects like anti-bunching have already been observed in the realm of quantum optics and this makes it an intriguing question how to find squeezed states and their effects in other places. In this context, few proposals have been suggested for the generation and detection of squeezed states of Bose-type excitations in solids.^{10,4,8,12} Quite recently, squeezed phonons have been produced and detected.⁹

It is very interesting that, unlike the case of light, the squeezed states of phonons may arise from different microscopic interactions in solids even at thermal equilibrium.⁴² Deviations from typical equilibrium distribution of phonons, namely Bose-Einstein distribution, might arise from anharmonic interactions among phonons or from some other mechanisms such as the polariton coupling in ionic crystals^{10,43} or polaron mechanism.⁴⁴ In such cases, equilibrium distribution of phonons are that of squeezed thermal phonons.¹⁵ Therefore, it seems to be an important question how to determine the equilibrium distribution of phonons when there is a possibility that phonons can be found to be in non-classical states. As a particular example of some considerable interest, the squeezed states of phonons due to the photon - optical phonon interaction in an ionic crystal⁴³ should be mentioned here. The polariton coupling in such a system is described by the following Hamiltonian⁴⁵

$$H = \frac{1}{2} \sum_k H_k,$$

$$H_k = \omega_k a_k^\dagger a_k + \omega_b b_k^\dagger b_k + ig_k [(a_k^\dagger - a_{-k})(b_k^\dagger + b_{-k}) + (a_{-k}^\dagger - a_k)(b_{-k} + b_k^\dagger)]$$

where ω_k is the photon frequency, ω_b is the frequency of transversal oscillations of optical phonons, g_k is the polariton coupling constant and the operators a_k, b_k describe the annihilation of photons and optical phonons respectively. Since the Hamiltonian under consideration is the Hermitian bilinear form, it can be

diagonalized by the Bogolubov canonical transformation⁴⁰ similar to that used in the definition of squeezed states.³⁹ As a result, the thermal equilibrium state of the system is described by the following density matrix

$$\rho(\beta) = \frac{e^{-\beta H_p}}{\text{Tr} e^{-\beta H_p}}$$

where H_p denotes the Hamiltonian H in diagonal (polariton) representation and β is the reciprocal temperature. In analogy to the quantum optics, we consider the so-called degree of coherence⁴⁶

$$G^{(2)} = \frac{\langle b^{\dagger 2} b^2 \rangle}{\langle b^{\dagger} b \rangle^2}$$

where $\langle \dots \rangle$ denotes the average with respect to the density matrix $\rho(\beta)$. It is straightforward to calculate $G^{(2)}$ as a function of temperature for typical parameters of an ionic crystal (see Fig.2.7). One can see that, at low temperatures, $G^{(2)} \approx 8$, while the same correlation function calculated with the Bose-Einstein distribution gives $G_{BE}^{(2)} = 2$. It is also seen that the strong quantum fluctuations can be observed only below $T \sim 50K$ because they are eroded by thermal fluctuations with the increase of temperature.

In contrast to the case of non-classical states of photons there is not any efficient direct method of measurement allowing the characterization of the quantum state of Bose-type excitations in solids.^{4,8} Even though correlation functions to any order would be demanded to describe fully a quantum state, it is usually good enough to distinguish quantum states by their number variances.⁴⁶ Here, we present a way to determine the number variance of phonons at equilibrium in a Raman active medium. It is already suggested that correlation Raman spectroscopy may be used to measure the quantum statistical properties of a vibration mode for the case of Stokes (S) type Raman scattering through a measurement of the intensity and the Mandel's Q-factor of the Rayleigh mode.⁴⁸ However, even at low temperatures vacuum fluctuations of the Anti-Stokes (AS) modes might disturb measurements of high order correlations and thus careful study of the role of the AS modes in such measurements is demanded. Here, we follow a similar ideology in more general terms by examining both the S

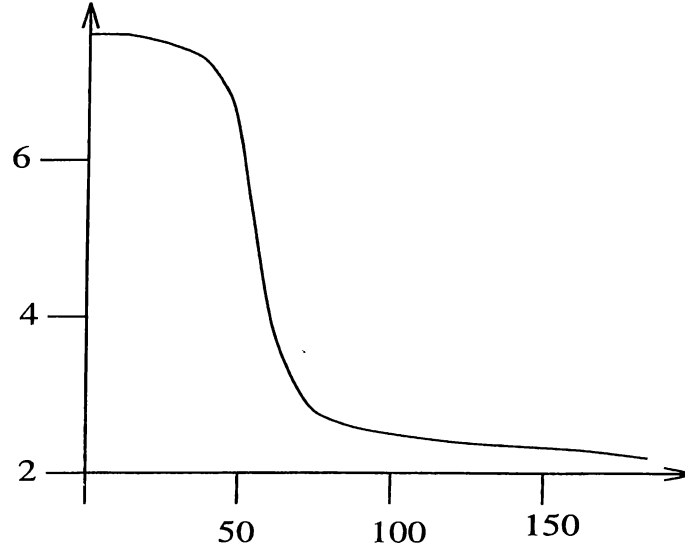


Figure 2.7: Phonon degree of coherence $G^{(2)}$ versus temperature for typical parameters of an ionic crystal: $\Omega = 200K$, $g = 25K$.

and AS components of multi-mode Raman scattering. Even though the problem becomes analytically intractable when AS modes are included, it is now possible to establish an interesting connection between the number variance of phonons and the correlations of S and AS modes. Moreover, due to the removing low temperature restriction in the exclusion of AS modes, influence of temperature in the high order quantum correlations can be examined as well.

2.2.2 Correlation of Stokes and anti-Stokes photons

General relations between the correlation function of S and AS modes and the number variance of phonons is developed in this section for the following Raman-type Hamiltonian,

$$H = \sum_{\mathbf{k}\lambda} \omega_{\mathbf{k}\lambda} a_{\mathbf{k}\lambda}^\dagger a_{\mathbf{k}\lambda} + \sum_{\mathbf{k}\mathbf{k}'\mathbf{q}} (M_{\mathbf{k}\mathbf{k}'\mathbf{q}}^S a_{\mathbf{k}'S}^\dagger a_{\mathbf{k}R} a_{\mathbf{q}V}^\dagger + M_{\mathbf{k}\mathbf{k}'\mathbf{q}}^A a_{\mathbf{k}'A}^\dagger a_{\mathbf{k}R} a_{\mathbf{q}V} + H.c.), \quad (2.21)$$

where $a_{\mathbf{k}\lambda}^\dagger$ ($a_{\mathbf{k}\lambda}$) are the creation (annihilation) operators for the λ -mode with momentum \mathbf{k} and corresponding frequency $\omega_{\mathbf{k}\lambda}$. Here the mode index $\lambda = S, A, V, R$ stands for Stokes, Anti-Stokes, vibration and Rayleigh modes,

respectively. The polarization labels are suppressed within the momentum symbols for the sake of notational simplicity. Coupling constants are denoted by $M_{\mathbf{k}\mathbf{k}'\mathbf{q}}^S$ for the S-type scattering and $M_{\mathbf{k}\mathbf{k}'\mathbf{q}}^A$ for the AS-type scattering. While writing this tri-linear bosonic Hamiltonian we assumed as usually⁵⁰ that the Raman scattering is observed under the condition $\omega_{R,S,A} \gg \omega_V$ when the pairwise creation of radiation modes has quite small probability so that energy is conserved. This supposition is equivalent to the rotating wave approximation of the quantum optics.⁴⁹ We also assumed that the radiation consists of three R , S , and AS pulses which are well-separated on the frequency domain so that $[a_{\mathbf{k}\lambda}, a_{\mathbf{k}'\lambda'}^\dagger] = \delta_{\mathbf{k}\mathbf{k}'}\delta_{\lambda\lambda'}$. If a single-mode strong coherent (classical) pumping is assumed, all one can expect is that the phase-matching conditions would have limited the number of active phonon modes to one. Nevertheless, it seems to be reasonable to consider the Raman scattering by an infinite Markoffian system of phonons.^{51,52} In particular, it permits one to take into account the broadening of S and AS lines. The usual selection rules of Raman scattering, namely phase-matching or quasi-resonance conditions,⁵⁰ are not essential for the derivation of the general relations below. Therefore, the results given in this section are also valid in not so perfect Raman coupling situations which should be important in real materials.

If we define the number operator $n_{\mathbf{k}\lambda}$ for the λ -mode with momentum \mathbf{k} as $n_{\mathbf{k}\lambda} = a_{\mathbf{k}\lambda}^\dagger a_{\mathbf{k}\lambda}$, then the total number operator N_λ for λ -mode becomes $N_\lambda = \sum_{\mathbf{k}} n_{\mathbf{k}\lambda}$. Heisenberg equations of motion yield the conservation laws, also known as Manley-Rowe relations,⁵⁰

$$N_S + N_A + N_R = C_1, \quad (2.22)$$

$$N_S - N_A - N_V = C_2.$$

Here constant operators C_1, C_2 are specified by the initial conditions. Similar relations can also be constructed for the scattering of photons of a monochromatic laser beam from a dispersionless optical phonon.^{53,42} Solving these equations for N_S and N_A , the S and AS correlation function is found to be

$$\langle N_A; N_S \rangle = \frac{1}{4}(V(C_1) - V(C_2) + V(N_R) - V(N_V))$$

$$-2 \langle C_1; N_R \rangle - 2 \langle C_2; N_V \rangle, \quad (2.23)$$

where the correlation function $\langle A; B \rangle$ of two operators A, B is defined by

$$\langle A; B \rangle = \langle AB \rangle - \langle A \rangle \langle B \rangle$$

and hence variance of operator A is given by the self-correlation function $V(A) = \langle A; A \rangle$. Here the averages $\langle . \rangle$ are with respect to the initial state since Heisenberg picture is used. It is natural to consider an initial state in which the S and AS modes are in their vacuum states, hence we obtain,

$$\begin{aligned} \langle N_A(t); N_S(t) \rangle &= \frac{1}{4} (V(N_R(0)) - V(N_V(0)) + V(N_R(t)) - V(N_V(t))) \\ &\quad - 2 \langle N_R(0); N_R(t) \rangle - 2 \langle N_V(0); N_V(t) \rangle. \end{aligned} \quad (2.24)$$

An operator A at time t is indicated by $A(t)$ while initially by $A(0)$. That equation connects the S and AS correlation function to the quantum statistical behavior of phonons and pump photons.

Within conventional Raman theory quantum properties of pump are usually neglected through the classical pump assumption.^{54,55} This approximation introduces a time range to the problem during which changes in the pump intensity remains negligible. We can apply a similar approximation by assuming an intense laser pump with photons in coherent states and performing a mean field average over them in the above equations. Under this assumption, the correlation function of the S and AS modes is related only to phonon statistics and the initial, known, number variance of the pump photons. However, time range of validity for the parametric approximation should be modified in our case. As we shall show in the subsequent section, statistical behavior of the pump might change significantly in shorter time than the occurrence of a significant change in its intensity. Our purpose is to examine the equilibrium statistics of phonons determined by $V(N_V(0))$; therefore we need to express all time dependent terms on the right hand side of the Eq.2.24, in terms of initial operators to see any further relation between the S and AS correlation function and the equilibrium variance of phonons. For that aim we specify a model system and study its dynamics.

We conclude this section by noting that a similar relation can be derived for the molecular Raman model, which is equivalent to the full bosonic Raman model under Holstein-Primakoff approximation in the case of low excitation density.⁵⁶ In that case, S and AS correlations depend on the quantum statistics of population distributions of the molecular energy levels.

2.2.3 Parametric Raman Model

In reality, coupling of one vibration mode to the pump beam for sufficiently long time of measurement is not an easy task. Therefore, in this section we investigate a Raman scattering in which coupling of pump photons to all phonon modes are allowed. We shall treat the pump as an intense coherent beam of photons and thus its state $|\psi_R\rangle$ in general is described by a multimode coherent state,

$$|\psi_R\rangle = \prod_{\mathbf{l}} \otimes |\alpha_{\mathbf{l}}\rangle \quad (2.25)$$

in which $\alpha_{\mathbf{l}}$ are the coherence parameters of the modes \mathbf{l} . According to the remarks at the end of previous section, we now perform mean field averaging with respect to pump photon states in Eq.1 assuming the Raman-active material is placed in an ideal cavity which selects single modes for S and AS radiations, namely $\mathbf{k}' = \mathbf{k}_{A,S}$. Then after dropping constant terms, the Hamiltonian reduces to an effective one,

$$H^{eff} = \sum_{\lambda=S,A} \omega_{\lambda} n_{\lambda} + \sum_{\mathbf{q}} \omega_{\mathbf{q}V} a_{\mathbf{q}V}^{\dagger} a_{\mathbf{q}V} + \sum_{\mathbf{q}} (g_{\mathbf{q}}^S a_S^{\dagger} a_{\mathbf{q}V}^{\dagger} + g_{\mathbf{q}}^A a_A^{\dagger} a_{\mathbf{q}V} + H.c.), \quad (2.26)$$

where new effective coupling constants $g_{\mathbf{q}}^{A,S}$ are introduced by

$$g_{\mathbf{q}}^{A,S} = \sum_{\mathbf{k}} M_{\mathbf{k}\mathbf{k}_{A,S}\mathbf{q}}^{A,S} \alpha_{\mathbf{k}} \quad (2.27)$$

The summation above can be calculated once the density of states for the pump is also specified. As one can see, the Hamiltonian will be in the given form, involving summations over phonon modes, in all cases except in the case of perfectly phase matched single pump and phonon modes. In order to make sure that our results

are not too susceptible to any imperfectness of the system arising from multi-mode nature of pump or phase-mismatches among the phonon and photon modes, we shall treat the problem using the model described by the above Hamiltonian involving summations over phonon modes, as a Markoffian bath system. When finite number of phonon modes are assumed, which is reasonable for real crystals of finite size, then such a model becomes integrable since the dynamics is ruled by the following closed set of operator linear differential equations,

$$\begin{aligned} i\frac{d}{dt}a_{\mathbf{q}V} &= \omega_{\mathbf{q}V}a_{\mathbf{q}V} + g_{\mathbf{q}}^S a_S^\dagger + g_{\mathbf{q}}^{A*} a_A, \\ i\frac{d}{dt}a_S^\dagger &= -\omega_S a_S^\dagger - \sum_{\mathbf{q}} g_{\mathbf{q}}^{S*} a_{\mathbf{q}V}, \\ i\frac{d}{dt}a_A &= \omega_A a_A + \sum_{\mathbf{q}} g_{\mathbf{q}}^A a_{\mathbf{q}V}. \end{aligned} \quad (2.28)$$

Let us introduce a vector of operators such that $Y = [a_S^\dagger, a_A, \{a_{\mathbf{q}V}\}]^T$. We denote the matrix of coefficients in the above set of equations by M and its diagonalizing matrix by D , so that $D^{-1}MD = E\mathbf{1}$ with eigenvalues E . Thus, we get

$$Y_i(t) = D_{ij} D_{jk}^{-1} Y_k(0) \exp(-iE_j t), \quad (2.29)$$

where summation over repeated index is implied. It is therefore possible to write the solution for $\lambda = S, A$ -modes in the form,

$$a_\lambda(t)^\dagger = u_\lambda(t) a_S^\dagger + v_\lambda(t) a_A + \sum_{\mathbf{q}} w_{\mathbf{q}\lambda}(t) a_{\mathbf{q}V}. \quad (2.30)$$

Operators without time arguments are taken at $t = 0$. Time dependent parameters u, v, w are determined by the elements of matrix D and eigenvalues E . Let us note here that some general relations exist among u, v, w due to the commutation relations for a_λ operators and they are not independent each other. More explicit way of evaluating u, v, w is presented below for the single mode phonon case where vector Y reduces to three dimensions in operator space. When there are no scattered light modes initially, the correlation function of S and AS modes becomes

$$\langle n_S(t); n_A(t) \rangle = A(t) + \sum_{\mathbf{k}\mathbf{q}} B_{\mathbf{k}\mathbf{q}}(t) \langle a_{\mathbf{k}V}^\dagger a_{\mathbf{q}V} \rangle + \sum_{\mathbf{k}\mathbf{l}\mathbf{p}\mathbf{q}} C_{\mathbf{k}\mathbf{l}\mathbf{p}\mathbf{q}}(t) \langle a_{\mathbf{k}V}^\dagger a_{\mathbf{q}V}; a_{\mathbf{l}V}^\dagger a_{\mathbf{p}V} \rangle \quad (2.31)$$

Here, parameters A, B, C are functions of u, v, w . Since the summations above can be converted into integrals involving phonon density of states, we see that if there are Van Hove singularities corresponding to the modes selected by Raman scattering, as in the case of recent experiments on the generation of non-classical phonon states via Raman scatterings,⁹ then the correlation of S and AS modes will be determined strongly by that mode. If this is not the case, then one can still expect domination of the modes obeying Raman selection rules. Then for that mode the random phase approximation permits us to write⁴⁷

$$\begin{aligned}\langle n_S(t) \rangle &= |v_S(t)|^2 + |w'_S|^2 (1 + n_V) \\ \langle n_A(t) \rangle &= |u_A(t)|^2 + |w'_A|^2 n_V \\ \langle n_S(t); n_A(t) \rangle &= A'(t) + B'(t)n_V + C'(t)V(n_V),\end{aligned}\tag{2.32}$$

in which the momentum label corresponding to relevant mode is fixed and dropped for the notational simplicity and primed parameters evaluated at that mode. It is possible to argue by the results above that a measurement of the correlation between S and AS can be utilized to determine the variance of vibration modes, which we usually consider as phonons here, provided one knows the mean number of such modes initially. The latter information can be determined by either one of the first two relations in Eq.2.28, after measurement of radiation mode intensities. Also measurement of radiation mode intensities and the knowledge of initial phonon number allow one to keep track of the evolution of mean phonon number through the Manley-Rowe relations. Interestingly, since the mean number of phonons with non-classical distributions deviate significantly from that of Bose-Einstein distribution, it might be possible to find some traces of non-classicality even here. However, in order to classify the distribution of phonons strictly it would still be necessary to find the next moment of the distribution, in other words the variance of phonons.

Now, an explicit way of determining u, v, w parameters will be demonstrated for the case of a single phonon mode. Because of three dimensional operator space in this situation, eigenvalues E_l are found to be as the roots of the cubic

equation

$$E^3 + 3\omega_V E^2 - [\omega_R^2 - 3\omega_V^2 + (|g^A|^2 - |g^S|^2)]E + [|g^S|^2(\omega_R + \omega_V) + |g^A|^2(\omega_R - \omega_V)] + \omega_V(\omega_V^2 - \omega_R^2) = 0.$$

Introducing coefficients P_l, Q_l as

$$P_l = -\frac{(E_l + \omega_V)(E_l + \omega_R + \omega_V) + |g^S|^2 - |g^A|^2}{2g^S \omega_R},$$

$$Q_l = -\frac{g^S P_l + E_l + \omega_V}{g^{A*}},$$

we write the field operators as

$$\hat{a}_S^\dagger(t) = \sum_l P_l A_l e^{iE_l t}, \quad (2.33)$$

$$\hat{a}_A(t) = \sum_l Q_l A_l e^{iE_l t}.$$

Common operator coefficients A_l are determined in terms of the operators $a_V(0), a_S^\dagger(0), a_A(0)$ using the Cramer's rule $\hat{A}_l = \det(D_l) / \det(D)$ where

$$D = \begin{pmatrix} 1 & 1 & 1 \\ P_1 & P_2 & P_3 \\ Q_1 & Q_2 & Q_3 \end{pmatrix}.$$

and D_l is the matrix obtained by replacing the elements in the l th column of D by the column vector $[\hat{a}_V(0), \hat{a}_S^\dagger(0), \hat{a}_A(0)]^T$. Thus, parameters u, v, w are determined in terms of interaction constants and the frequencies. More explicit expressions are too long and not very illuminating to reproduce here, but above analysis is quite suitable for numerical computation when some experimental data is available. At that moment we shall content ourselves with more fundamental discussions only.

In order to give a brief discussion of the dependence of the correlation function in Eq.9 on squeezing parameter and temperature, we consider an equilibrium distribution of vibration mode as of the squeezed thermal state with the following

mean number and number variance¹⁵

$$\begin{aligned}\langle n_V \rangle &= \bar{n}_V \cosh 2r + \sinh^2 r, \\ V_0(n_V) &= (\bar{n}_V^2 + \bar{n}_V) \cosh 4r + \frac{1}{2} \sinh^2 2r,\end{aligned}\quad (2.34)$$

where \bar{n}_V is the mean number of phonons according to Bose-Einstein (BE) distribution and r is the real squeezing parameter. When $r = 0$, we recover the usual BE-distribution. According to Eq.2.28, the S and AS correlations increases with variance of phonons. And since both the n_V and the $V(n_V)$ increases with temperature, we see that temperature enforces stronger correlations of S and AS modes. However, we need to put a word of caution here, since the fluctuations which are determined by the self-correlations of the modes also increases with the temperature. In order to represent this competition, one can consider the cross-correlation function defined by⁵⁷

$$C_{S-AS} = \frac{\langle n_S, n_A \rangle}{\sqrt{V(n_S)V(n_A)}}. \quad (2.35)$$

Since the denominator can be expressed in a similar structure as with the correlation function in Eq.2.28, the cross correlation function will eventually saturate at high temperatures and at high squeezing parameters. Therefore, at high temperatures thermal fluctuations becomes important but not more important than in any typical quantum measurement. An estimation for a typical ionic crystal, for example, shows that the level of quantum fluctuations of phonon number exceeds that of thermal fluctuations below $30 \div 50\text{K}$.^{42,43} We also see that S and AS correlation increases with the squeezing parameter r .

Finally, we examine the time range of validity for the parametric approximation. For that aim, we consider the Hamiltonian for the case of perfect coupling of single modes. Let us suppress the momentum within the mode labels R, S, V, A and calculate $a_R(t)$ for times close to the beginning of interaction.⁵⁸ Up to the second order, we get

$$a_R(t) = e^{-i\omega_R t} (a_R + it(M^{S*} a_S a_V + M^{A*} a_A a_V^\dagger) - \frac{1}{2} t^2 (|M^S|^2 \nu + |M^A|^2 \mu)) \quad (2.36)$$

where $\nu = a_R(n_S + n_V + 1)$, $\mu = a_R(n_A - n_V)$. Here, operators at $t = 0$ are those without time arguments. Then, we calculate the mean number and the variance of pump photons for S and AS modes are in vacuum states initially as

$$\begin{aligned} n_R(t) &= n_R - t^2(|M^S|^2 n_R(1 + n_V) + |M^A|^2 n_R n_S), \\ V(n_R(t)) &= V(n_R) + 2t^2(|M^S|^2(V(n_R)(1 + n_V) + n_R(1 + n_V) + \\ &+ |M^A|^2(V(n_R)n_V - n_R n_V))) \end{aligned} \quad (2.37)$$

In these equations averaging symbol, $\langle . \rangle$, is not shown. Using the relation $V(n_R) = n_R$ for a coherent field, we find the time ranges $t \ll \tau_1, \tau_2$, for which the field intensity and the variance remain close to their initial values, as

$$\begin{aligned} \tau_1 &= \frac{1}{|M^S|^2(1 + n_V) + |M^A|^2 n_V}, \\ \tau_2 &= \frac{1}{4|M^S|^2(1 + n_V)}. \end{aligned} \quad (2.38)$$

Clearly, we see a rescaling of time range of the usual time range of parametric approximation. At low temperatures $n_V \approx 0$ and thus $\tau_2 = (1/4)\tau_1$ shows a reduction of time range to 1/4 of the typical range of parametric approximation. As an estimation, we may take $g^S \approx 10^7 Hz$,⁵⁸ giving time ranges as $\tau_1 = 10fs$ and $\tau_2 = 2.5fs$. These ranges are readily available due to the remarkable recent developments in the field of femto-second spectroscopy.^{59,60}

2.2.4 Summary

Summing up our results, we should stress that the measurement of Stokes–anti-Stokes correlations looks like a reasonable method for detecting the number variance of a Raman-active vibration mode in solids. The most interesting and crucial fact is that the above method permits us to determine the number variance at thermal equilibrium, in other words, the variance just before the application of the pump beam. The phonon sub-system could be in a non-classical state due to an interaction providing necessary correlations among phonons before the pump beam is applied. That interaction could be some anharmonic coupling

with the heat bath, polaron or polariton mechanisms. Since these mechanisms are usually weaker than the first order Raman effect, after the application of the pump beam, dynamics of the phonon system is governed mainly by the Raman effect. Therefore, initial non-classical state of phonons and non-classical effects like squeezing which require phase coherence might be destroyed. That is why we have determined the general and fundamental formula given by Eq.2.20, in terms of the initial state of phonons and showed that under certain conditions it provides direct information on the initial, thermal equilibrium variance of phonons. Analyzing those conditions of applicability, we propose that at liquid N_2 temperatures, using an intense coherent beam of ultra-fast laser source such as *Ti*-sapphire as a pump for a Raman active medium, one can measure the number correlation of the scattered Stokes and anti-Stokes modes and the mean photon numbers in these modes simultaneously by some photon counters, in order to determine the number variance of the vibration mode at equilibrium. The measurement can be realized through the use of a homodyne-type scheme⁴⁶ in which the S and AS photons are counted by two different detectors connected to a computer fixing the simultaneous arrival of the S and AS photons. It is also shown that when the vibration mode is in squeezed state then an increase in the correlation of the Stokes and anti-Stokes modes occurs.

Case of a multi-mode pump, important for ultra-short pulses, can be handled easily for materials which involves a strongly preferred phonon mode due to a Van Hove singularity in the frequency range of the pump, by an appropriate calculation of the effective coupling constants which in turn modify only the coefficients A', B', C' . Thus our conclusions should also be valid in this case. For materials in which such phonon modes are many or not exists at all, then application of a multi-mode pump and measurement of Stokes-Anti-Stokes correlation would still provide information on multi-mode phonon correlations according to the general formula. This is a valuable knowledge to classify a possible non-classical multi-mode state of phonons like a multi-mode squeezed state.

So far, the best achievement in squeezing of phonons is reported to be 0.01%,⁹

provided by second order Raman scattering. We would like to emphasize that this is not the squeezing parameter r but related to $V(n_V)$. Hence, the change in the Stokes–Anti-Stokes correlations we expect to be in the same order. There are other mechanisms which result in non-classical excitations in solids with different expressions and larger values for r and $V(n)$. In fact, squeezing parameter reflects the strength of interaction preparing the non-classical state of these excitations,^{4,8} which is the initial phonon state in our scheme. The example of optical polariton we have discussed in the introduction, provides a two-mode squeezed state with squeezing parameter in the range $r \sim 0.1 - 0.01$ in *CuCl*.¹⁰ Therefore, such a measurement with the ultrafast Raman correlation spectroscopy should not be too challenging and looks promising in our opinion.

Let us finally note that the case of molecular Raman spectroscopy can also be treated with a similar formalism to get information on the quantum statistics of populations of molecular energy levels.

Chapter 3

Theory of Polarization

This chapter will begin by a detailed review of vector spherical harmonics. They provide a natural basis for examination of the multipole radiation of localized sources. Therefore, study of their properties is essential for further understanding of the properties of multipole radiation, in particular comprehending vector nature of spherical harmonics in this context, will be very useful for interpreting polarization properties of multipole radiation. We will follow the treatment by Arfken⁶¹ in the presentation of vector spherical harmonics in a concise yet comprehensible and complete way.

3.1 Vector Spherical Harmonics

In many electrodynamic phenomena one usually encounters vector differential equations in the form,

$$\nabla \times \nabla \times A = \mu_0 J, \quad (3.1)$$

where A is the vector potential and J is the current density. Due to the vector nature of this equation, three scalar equations corresponding to scalar components of the vector fields A and J can be obtained. If boundary conditions are specified in spherical components, then three equations would involve A_r , A_θ and A_ϕ components, and the equations would be coupled. Though they can be

solved, the process is usually rather involved and formidable.

In order to solve the electrodynamical vector differential equations, one also need to consider an appropriate gauge for the problem. In optical radiation problems, we usually use a gauge in which

$$\nabla \cdot A = 0. \quad (3.2)$$

This gauge is called in literature with different names: transversal gauge, radiation gauge, and Coulomb gauge. Here, we adopt the term transversal gauge. In this gauge, differential equation becomes,

$$\nabla^2 A + \mu_0 J = 0. \quad (3.3)$$

At first sight, we recognize that, choice of scalar components of vector potential as Cartesian components would yield three uncoupled equations. Eventhough, this looks a great simplification, unfortunately for boundary conditions expressed in spherical components involve mixture of Cartesian components and this would ruin all the promised simplicity. In order to deal with boundary conditions in a simple manner, we would need a set of complete solutions which would reflect the symmetry of the problem imposed by the boundary conditions. E. H. Hill, in his "Theory of Vector Spherical Harmonics" introduced one such set in early fifties.⁶² Using the Condon-Shortley phase convention, he introduces

$$V_{jm} = \frac{1}{2j+1} \left\{ -e_r \sqrt{j+1} Y_{jm} + e_\theta \frac{1}{j+1} \frac{\partial Y_{jm}}{\partial \theta} + ime_\phi \frac{1}{\sqrt{j+1} \sin \theta} Y_{jm} \right\}, \quad (3.4)$$

$$W_{jm} = \frac{1}{2j+1} \left\{ e_r \sqrt{j} Y_{jm} + e_\theta \frac{1}{j} \frac{\partial Y_{jm}}{\partial \theta} + ime_\phi \frac{1}{\sqrt{j} \sin \theta} Y_{jm} \right\}, \quad (3.5)$$

$$X_{jm} = \frac{1}{2j+1} \left\{ -me_\theta \frac{1}{\sqrt{j} \sin \theta} Y_{jm} - ie_\phi \frac{1}{j} \frac{\partial Y_{jm}}{\partial \theta} \right\}. \quad (3.6)$$

Here e_r, e_θ, e_ϕ are unit vectors in spherical coordinates, and Y_{jm} are scalar spherical harmonics. Well known properties of scalar spherical harmonics can

be used to prove and derive similar properties for vector spherical harmonics. Since, scalar spherical harmonics are orthogonal with,

$$\int d\Omega Y_{j'm'}^* Y_{jm} = \delta_{j'j} \delta_{m'm}, \quad (3.7)$$

it can be shown that vector spherical harmonics also satisfy a similar orthogonality relation

$$\int d\Omega F_{j'm'}^* G_{jm} = \delta_{j'j} \delta_{m'm}, \quad (3.8)$$

where F and G stand for V, W or X . Using the sum rule for scalar spherical harmonics, similar rules can be obtained for vector spherical harmonics, too. For example,

$$\sum_{m=-j}^j X_{jm}^* X_{jm} = \frac{2j+1}{4\pi}, \quad (3.9)$$

Note that, most problems we will deal with involve X vector spherical harmonics because of the transversal gauge. This can be seen from the following differential relations,

$$\nabla \cdot (f(r)V_{jm}) = -\sqrt{\frac{j+1}{2j+1}} \left(\frac{df}{dr} + \frac{j+2}{r} f \right) Y_{jm}, \quad (3.10)$$

$$\nabla \cdot (f(r)W_{jm}) = \sqrt{\frac{j}{2j+1}} \left(\frac{df}{dr} - \frac{j-1}{r} f \right) Y_{jm}, \quad (3.11)$$

$$\nabla \cdot (f(r)X_{jm}) = 0. \quad (3.12)$$

Then, in transversal gauge, and taking $J = 0$ for source-free region, i.e. away from the source currents, and using $A = f(r)X_{jm}$ we obtain after calculating $\nabla^2 A = 0$,

$$\nabla^2 (f(r)X_{jm}) = \left(\frac{df}{dr^2} + \frac{2}{r} \frac{df}{dr} - \frac{j+2}{r} f \right) X_{jm} = 0. \quad (3.13)$$

Therefore, the general solution is

$$A_{jm} = a_{jm} r^{-j-1} X_{jm} \quad (3.14)$$

For illustration, considering a current loop, we see that $m = 0$ in this case and the solution reduces to

$$A_j = a_j r^{-j-1} \left[\frac{-i}{\sqrt{j(j+1)}} \frac{\partial Y_{j0}}{\partial \theta} \right] e_\phi, \quad (3.15)$$

in agreement with the solutions obtained by other methods. We will also note a particularly useful differential relation for X function, namely the curl relation,

$$\begin{aligned} \nabla \times f(r) X_{jm} &= i \sqrt{\frac{j}{2j+1}} \left(\frac{df}{dr} - \frac{j}{r} \right) V_{jm} \\ &\quad + i \sqrt{\frac{j+1}{2j+1}} \left(\frac{df}{dr} + \frac{j+1}{r} \right) W_{jm}. \end{aligned} \quad (3.16)$$

Another frequently encountered integral relation is,

$$\int d\Omega X_{jm} \cdot (r \times X_{jm}) = 0. \quad (3.17)$$

For completeness, let us also note the parity relations,

$$V_{jm}(\theta', \phi') = (-1)^{j+1} V_{jm}(\theta, \phi), \quad (3.18)$$

$$W_{jm}(\theta', \phi') = (-1)^{j+1} W_{jm}(\theta, \phi), \quad (3.19)$$

$$X_{jm}(\theta', \phi') = (-1)^j X_{jm}(\theta, \phi), \quad (3.20)$$

with $\theta' = \pi - \theta$ and $\phi' = \pi + \phi$. For our purposes, it will be nice to express vector spherical harmonics in a more physical way. By direct calculation it can be shown that vector spherical harmonic X_{jm} can be written in connection with the orbital angular momentum,³¹ i.e.,

$$X_{jm} = \frac{1}{\sqrt{j(j+1)}} L Y_{jm}. \quad (3.21)$$

Power of this representation will be clear when we use quantum mechanical treatment; since, angular momentum is a significant parameter in quantum theory. We will also exploit this, in order to separate the longitudinal and transverse components of the radiation in a similar manner described by Morse and Feshbach.⁶³ It must be noted that, applications of vector spherical harmonics

in radiation problems is not limited to optical problems. More uses and other applications can be found in literature.⁶⁴ In fact, developing vector spherical harmonics, alternatively by addition of angular momentum allows generalizing their concept to tensor spherical harmonics. For instance, vector spherical harmonics can be constructed through coupling j units of orbital angular momentum to 1 unit of spin angular momentum. If we consider coupling of j units of orbital angular momentum to 2 units of spin angular momentum, then we would obtain the tensor spherical harmonics. They are used in the description of gravitational radiation by J. Matthews.⁶⁵ We will proceed by using them as a natural basis for description of classical³¹ and quantum⁶⁶ multipole radiation in the Bouwkamp-Casimir formalism.⁶⁷ Similar construction of quantum theory of radiation was also given by Heitler's quantum theory of radiation.³²

3.2 Multipole Expansion of Electromagnetic Fields

In this section we will construct multipole expansion of electromagnetic fields radiating from localized charge and current distributions. Our emphasis will be on electric charge distributions, since they are important as being the atomic sources of radiation, which lie at the heart of atomic and molecular optical physics and quantum optics. Before giving the full treatment of the propagation of radiation problem in the source free region, we will describe general ideology behind source-free approximation as well as we will clarify the frequently used terms in the treatment, including zones of radiation and the concept of localized source.

3.2.1 General overview of evolution of radiation

Any radiation problem, not only light radiation, should have three basic steps of evolution. First, it has a source. In the case of light, these are accelerated charges, current distributions, or in more macroscopic terms incoherent sources like stars, thermal electric bulbs, or coherent sources like lasers. In the case

of other radiations, like nuclear or gravitational radiation there are sources of radiation, too. These can include nuclear collisions, fission, nuclear decays, supernova bursts, black body formations, collapse of stars. Generation step is followed by, in general terms, propagation of that generated radiation, as a disturbance in space-time. For example, gravitational waves propagate as ripples in the curvature of space-time, light evolves as an electromagnetic field. It can be seen that radiation in most cases generated through an interaction, and like any interaction that generation process has also a range. After the limits of the range of generating interaction, effects of this interaction is considered to be negligible. Therefore, propagation region, which starts just beyond the range of generating interaction is considered to be source-free region. And, thus the radiation evolves as a free radiation field in the propagation region. In most cases, especially for the light and gravitational radiation this is very good approximation. Finally, for practical purposes we introduce a detection, or absorption region. Here, the radiation is detected and measurements are performed, or indirect and direct effects are observed. This general picture is illustrated in Fig.3.1.

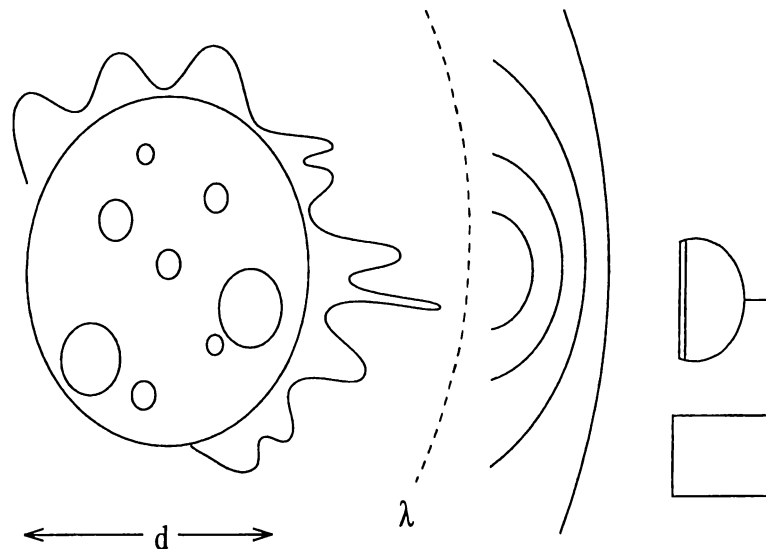


Figure 3.1: Evolution of radiation, different spatial behaviors at different zones (stages) are illustrated.

3.2.2 Localized sources of radiation

Our focus throughout in this work, will be on electromagnetic radiation generated by a closed system of oscillating charges. By that, we mean there is no loss of charge during the generation process. Moreover, we will consider that this system of charges can be confined within an effective sphere of radius d , as indicated in Fig.3.1, even though the shape of the system doesn't have to be a sphere at all. This effective size of the system will be considered much smaller than any length of interest in the propagation problem. A source with these specifications is called as a localized source. There is a growth of interest in modern optics for these sources. While antennas, like center-fed linear antenna, are also examples of multipole radiation, recent developments in atomic physics, as well as mezosopic physics, allow even more smaller confinement regions for radiation sources. Remarkable ones include electrons confined in quantum wells, and atoms, or ions confined in ion-atom traps. Significance of such sources stems from the fact that quantum computers and quantum communication and teleportation sources demand such small and localized sources. In other words, such trapped atoms and electrons can be realized as chips in quantum optical computers of the next century.

3.2.3 Zones of radiation

We have seen that assuming the separation of generation and propagation regions is possible, we can treat the evolution of radiation in the propagation region as a source-free evolution. In theory, this offers great simplification of the problem. However, it is also possible to look for even more simple view of the problem. This is achieved by recognizing that most of the detection and measurement on the radiation field is usually done very far away from the source. Near the source, as well as in places where wavelength of the radiation is comparable to the distance to the source, radiation field exhibit quite complicated behavior than when it is far away from the source. Then, we further sub-divide the propagation region into three zones. In each zone, radiation field posses certain characteristics, and they are qualitatively as well as quantitatively different than the ones in other

zones. Critical parameter in the separation of the zones is the wavelength, λ of the radiation. Then we introduce the following zones:

- Generation Zone: $0 < r < d$
- Near Zone: $d \ll r \ll \lambda$
- Intermediate Zone: $d \ll r \sim \lambda$
- Far Zone: $d \ll \lambda \ll r$

In each zone, radiation field show characteristically different behaviors. For multipole radiation of localized sources, near zone field has also local character. In other words, some part of the radiated field sticks to a region near the zone, and cannot escape far away from the source. On the other hand, radiated field has some components which can reach outer space, i.e. beyond the λ limit, and can be detected. In optics, we usually deal with those propagating components. Fig.3.1 also points out local component near the source as an aurora around the source. It also demonstrated spherical wave fronts of propagating field components in the far zone. From theoretical point of view, such zone separation permits us to use asymptotic forms of spatial functions for the otherwise highly complicated electromagnetic field functions.

3.2.4 Different zone behaviors illustrated:dipole radiation

Dipole radiation is most common, and important multipole radiation. One reason is its theoretical simplicity, and another reason is that it is the strongest radiation, and easier to observe. Besides, it is related to two level systems of quantum optics, including Jaynes-Cummings model. These models are very important on information coding in two level systems in terms of logical 1_L and logical 0_L . In quantum computing language, they are called as qubits. Therefore, it is necessary to devote a separate section to discuss properties of dipole radiation and comparison of behaviors in different zones. Note that, these properties will also quite similar for the case of a general multipole radiation.

Electric dipole moment is defined by,

$$\vec{p} = \int \vec{r}' \rho(\vec{r}') d^3\vec{r}'. \quad (3.22)$$

Then the vector potential is found to be

$$\vec{A}(\vec{r}) = -ik\vec{p}\frac{e^{ikr}}{r}. \quad (3.23)$$

Using the vector potential, electric and magnetic fields for the dipole radiation are calculated and they are obtained as,

$$\begin{aligned} \vec{B} &= \vec{\nabla} \times \vec{A} = k^2(\vec{n} \times \vec{p})\frac{e^{ikr}}{r}\left(1 - \frac{1}{ikr}\right), \\ \vec{E} &= \frac{i}{k}\vec{\nabla} \times \vec{B} \\ &= k^2(\vec{n} \times \vec{p}) \times \vec{n}\frac{e^{ikr}}{r} + [3\vec{n}(\vec{n} \cdot \vec{p}) - \vec{p}]\left(\frac{1}{r^3} - \frac{ik}{r^2}\right)e^{ikr} \end{aligned}$$

This result is exact, and valid in all zones of radiation. It describes well for the radiation in the intermediate region. However, we don't need to use this full form in far and near zones. We can single out dominating terms and obtain simpler and more illustrative result for these asymptotic regions. Using $kr \ll 1$ in near zone and $kr \gg 1$ in far zone, we simplify the above general expression for these zones. In far zone, fields turn out to be in the following form,

$$\vec{B} = k^2(\vec{n} \times \vec{p})e^{ikr}/r, \quad (3.24)$$

$$\vec{E} = \vec{B} \times \vec{n}, \quad (3.25)$$

and in near zone they can be expressed as,

$$\vec{B} = ik(\vec{n} \times \vec{p})/r^2 \quad (3.26)$$

$$\vec{E} = [3\vec{n}(\vec{n} \cdot \vec{p}) - \vec{p}]/r^3. \quad (3.27)$$

Then we recognize the following differences:

1. Above expressions clearly indicate that fields have very different spatial behavior in near and far zones. In near zone, $B \sim r^{-2}$, $E \sim r^{-3}$ while in far zone $E, B \sim r^{-1}$. r^{-1} behavior is typical for radiation fields. Having both E and B have similar spatial dependence also indicates well defined light illumination.

2. In far zone e^{ikr}/r behavior represents an outgoing spherical wave. While, in near zone expression is exactly the same with electrostatic dipole solution. Therefore, near zone field is quasi-static. Quasi, since it has $e^{-i\omega t}$ oscillating temporal behavior.
3. Electric and magnetic field has same order of magnitude contribution to the field at far zone, $O[B/E] = 1$. However, in near zone field is dominated by the electric field, $O[B/E] = kr$.
4. Far zone fields are transversal to the propagation direction. But, in near zone electric field has a component along the direction of propagation. On the other hand magnetic field is again transversal. This hints that description of polarization as the direction of electric field has a local character and zone dependent. In far zone, polarization basis is two dimensional and transversal. While in near zone, due to the existence of longitudinal component it should be three dimensional.

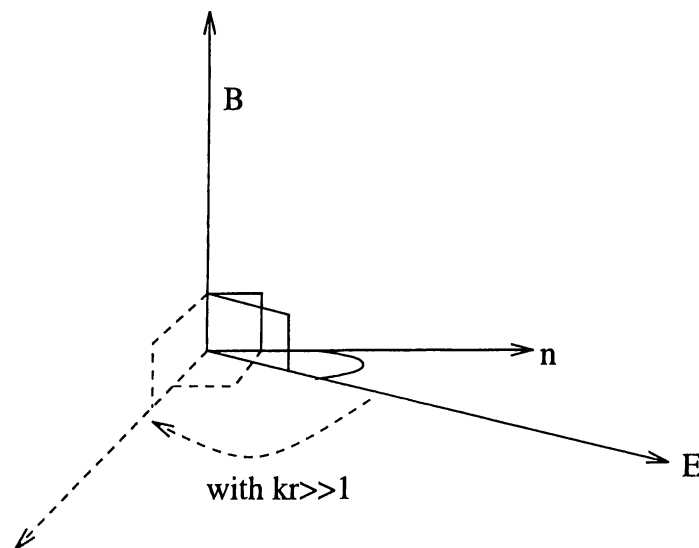


Figure 3.2: Change of direction of electric field as radiation propagates

We indicate in Fig.3.2 the change of the direction of electric field as radiation evolves from near zone to far zone, in other words as kr increases. Electric field

rotates about the B as increasing kr and becomes transversal finally at the far zone. This also shows change of polarization in different zones of radiation.

3.3 Standard Classical Theory of Polarization

We have seen that electric field is not always transversal when we considered dipole radiation example. Later, we will see that this is also true for more general multipole radiation. Nevertheless, the main difference is the existence of longitudinal component in the near and intermediate zones. If we are far enough from the source, better to say, if we are doing measurements at distances much greater than the wavelength of interest, than we can forget about that longitudinal component. Since the beginning of optical science, measurements are performed in far zone using the classical light. And polarization always considered to be a transversal property described in two dimensional basis. The story goes back to 1850s, and Prof. Stokes gives one of the first systematic study of polarization using intensity measurements. Surprisingly, his theory and Stokes parameters survived even today, and used for analysis of even quantum light and photons. We will discuss its validity for quantum light later. For now, let us review briefly old tools of polarization study and ellipsometry.

3.3.1 Poincaré Sphere

A beautiful representation of polarization states of light can be given by Poincaré sphere representation. In Fig.3.3, every point on the spherical surface corresponds to a polarization state. Poles of the sphere stand for circular polarization. Equatorial plane involves linear polarization states, between the poles and the equatorial planes lie the ellipsoidal polarization states. Right handed polarization states are those at the northern hemisphere and the left handed ones are those at the southern hemisphere. Using stereographical projection, it is possible to map spherical surface to a plane as shown in Fig.3.3. This beautiful picture of polarization unfortunately is only valid for transversal

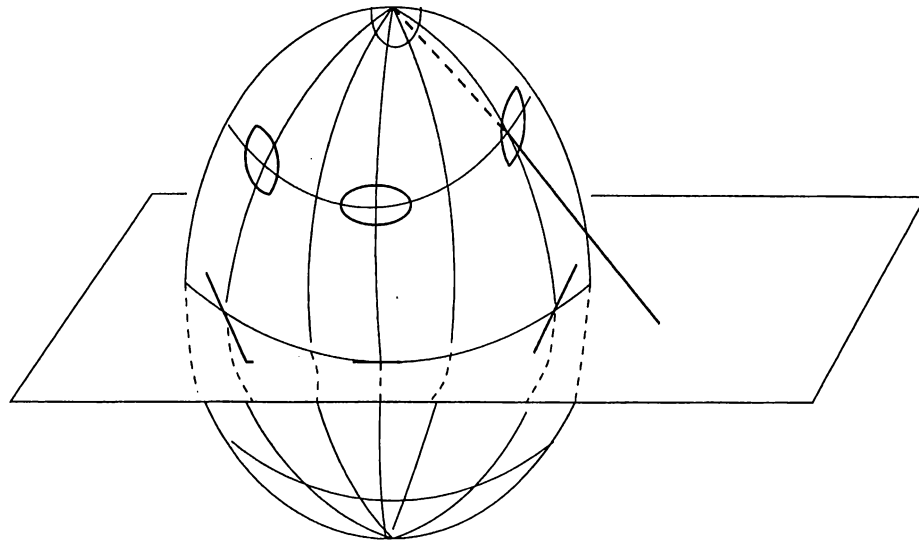


Figure 3.3: Poincaré sphere representation of transversal polarization states

polarization in the far zone. For a more global description of polarization in which longitudinal component also present, one would expect a more general hypersphere representation and a similar generalized stereographical projection would map that hypersphere-which we would expect to be four dimensional sphere-to an ordinary sphere. Interestingly, Poincaré sphere can also be used for quantum description of polarization. In terms of photons, unpolarized light can be understood as a uniform photon distribution over the Poincaré sphere, as photons always have polarization in contrast to the whole light beam. Partially polarized light can be understood as photon distribution has preferable regions over the sphere. While fully polarized light would have photons all located at the same point on the sphere. On the other hand, we will not focus on Poincaré sphere representation for global theory of polarization. Hypersphere would not be easy to visualize and would not be as useful as for the case of transversal polarization states.

3.3.2 Operational approach to polarization

Even though geometry is beautiful, we cannot easily see generalizations for a theory using it. Interestingly, most geometrical objects can also be associated with algebraic objects, namely matrices. Such connection and algebraic description is useful for generalization of ideas, and allows more systematic study of a theory. In mechanics as well as in optics, earlier studies are mostly geometrical. One can see this by looking through famous works of Newton, Principia and works by Faraday on field and potential lines. However more distance is covered in these fields after making connection to algebra and differential equations. In the case of optics and ellipsometry, as the study of polarization, Poincaré representation therefore is not much used, but the following construction, namely Jones matrix, or coherency matrix is used mostly.

$$J = \begin{pmatrix} \langle E_+ E_+^* \rangle & \langle E_+ E_-^* \rangle \\ \langle E_- E_+^* \rangle & \langle E_- E_-^* \rangle \end{pmatrix} \quad (3.28)$$

$$= \begin{pmatrix} J_{++} & J_{+-} \\ J_{-+} & J_{--} \end{pmatrix}. \quad (3.29)$$

Elements of this matrix constructed by tensor product of an electric field written in circular polarization basis,

$$E = (E_+ e_+ + E_- e_-) e^{ikz - i\omega t}, \quad (3.30)$$

with e_{\pm} are the circular polarization basis unit vectors, ω is the frequency and k is the wavevector of the planewave. Direction of propagation is taken to be the z axis. Averaging symbol in the elements of the coherency matrix takes into account the possibility of quasimonochromatic electromagnetic fields. In this case, we need to consider the complex amplitudes E_{\pm} vary slowly in time, when compared with frequency ω . Therefore, the brackets $\langle \rangle$ stand for macroscopic time average. We see that the elements of the coherency matrix have all the information we need to determine the polarization state of the light. Diagonal elements are just the intensities of different polarization components while off diagonal elements have the relative phase information. Another useful

representation of polarization states is given by Stokes, in terms of Stokes vector. Actually, they are just physical combinations of elements of coherency matrix. Components of Stokes vector are called as Stokes parameters.

$$\vec{S} = \begin{pmatrix} S_0 \\ S_1 \\ S_2 \\ S_3 \end{pmatrix} = \begin{pmatrix} J_{++} + J_{--} \\ J_{+-} + J_{-+} \\ i(J_{+-} - J_{-+}) \\ J_{++} - J_{--} \end{pmatrix} \quad (3.31)$$

More explicitly, Stokes parameters are given by,

$$\vec{S} = \begin{pmatrix} S_0 \\ S_1 \\ S_2 \\ S_3 \end{pmatrix} = \begin{pmatrix} \langle |E_+|^2 + |E_-|^2 \rangle \\ \langle 2\text{Re}(E_+^* E_-) \rangle \\ \langle 2\text{Im}(E_+^* E_-) \rangle \\ \langle |E_+|^2 - |E_-|^2 \rangle \end{pmatrix} \quad (3.32)$$

Here, the parameter S_0 measures the intensity of the wave. The parameter S_3 gives the preponderance of positive helicity (right handed circular polarization) component over the negative helicity (left handed circular polarization) component. Other parameters, S_1 and S_2 contain the phase information. It can be shown that S_1 is proportional to the *cosine* of the relative phase and S_2 is proportional to the *sine* of the relative phase. Therefore, knowing both of them, one can exactly determine the relative phase. In fact, there are three physical unknowns. Two are intensities, and one is the relative phase. Then we see that four Stokes operators are overdetermine the polarization information. They are actually not independent each other, and we have

$$S_0^2 \geq S_1^2 + S_2^2 + S_3^2. \quad (3.33)$$

For a monochromatic light, equality holds. For a quasimonochromatic light we have the inequality. Note that, 'natural light' has $S_1 = S_2 = S_3 = 0$. It might be noted here that, Stokes parameters are also used in astrophysical and other polarized radiation problems. Further discussions can be found in Born and Wolf.²⁹ In order to measure above introduced Stokes parameters,

we need to resort intensity measurements. Therefore, using simple rotational transformations, Stokes operators can be written as expressions in terms of intensities of polarized light.

$$\vec{S} = \begin{pmatrix} S_0 \\ S_1 \\ S_2 \\ S_3 \end{pmatrix} = \begin{pmatrix} I_0 \\ I_{+\frac{\pi}{4}} - I_{-\frac{\pi}{4}} \\ I_L - I_R \\ I_+ - I_- \end{pmatrix} \quad (3.34)$$

Here, I_0 is the total intensity, $I_{\pm\frac{\pi}{4}}$ are intensities of $\pm\pi/4$ linearly polarized lights, I_{\pm} are the intensities of lights with positive and negative helicity, and $I_{L,R}$ are linear polarized light intensities with vertical and horizontal polarizations. As one can imagine, by light polarizers along the path of light, all Stokes operators can easily be measured.

3.4 Standard Quantum Theory of Polarization

Stokes operators have been used since 1850s successfully, in order to determine the polarization state of the classical light. After the invention of laser and the beginning of modern era of quantum optics, very low intensity light, as well as ultrashort pulses became available. This opened a new way of looking optical phenomena in terms of photons, which are the quantum particles of electromagnetic fields. However, photons as quantum particles need to be described in terms of a set quantum numbers, like linear momentum, energy, angular momentum, spin, and so on. In this context, definition of polarization as the direction of electric field of the electromagnetic radiation seems not so clear from the point of view of photons. Then it becomes a delicate and intriguing question how to associate polarization of light to photon picture. Standard and conventional way to do this in literature is direct second quantization of Stokes parameters to obtain Stokes operators. Then since these operators are quadratic forms, they are diagonalized to be written in intensity, or number operator, expressions. Thus, by photon counting measurements they could be measured

and polarization information of light can still be deduced using photons even in the case of low intensity, quantum light. However, as we shall see this hope and ideology fails from several points. Electric field operator in second quantized form can be written as,

$$\vec{E} = i\sqrt{\frac{\hbar\omega}{\epsilon_0 V}}(\hat{a}_+\vec{e}_+ + \hat{a}_-\vec{e}_-)e^{i(kz-\omega t)} \quad (3.35)$$

As one can see this is actually the positive frequency part of the electric field, as it contains only the photon annihilation operators a_{\pm} . Here, V is the quantization volume. We consider it a very large cubic box of volume V and impose periodical boundary conditions for the fields. This translational invariance, brings conservation of linear momentum and also plane waves as the representations of translational group with linear momentum is its generator. The coefficient in front can be interpreted as electric field per photon. In fact, it is a rescaling that we need to bring photon picture through ladder operators of Weyl-Heisenberg algebra. Then using this electric field operator in Stokes parameters, we can immediately obtain the following set of Stokes operators,

$$\hat{S}_0 = \hat{a}_+^\dagger \hat{a}_+ + \hat{a}_-^\dagger \hat{a}_- \quad (3.36)$$

$$\hat{S}_1 = \hat{a}_+^\dagger \hat{a}_- + \hat{a}_-^\dagger \hat{a}_+ \quad (3.37)$$

$$\hat{S}_2 = i(\hat{a}_+^\dagger \hat{a}_- - \hat{a}_-^\dagger \hat{a}_+) \quad (3.38)$$

$$\hat{S}_3 = \hat{a}_+^\dagger \hat{a}_+ - \hat{a}_-^\dagger \hat{a}_- \quad (3.39)$$

Good point with these operators is that, they are quadratic in photon creation and annihilation operators. Therefore, it is possible to find a Bogolubov transformation to diagonalize each of them. Let us illustrate the diagonalization of Stokes operator S_1 . For that aim, it is useful to write it in quadratic form,

$$S_1 = (a_+^\dagger, a_-^\dagger) \begin{pmatrix} 0 & 1 \\ 1 & 0 \end{pmatrix} \begin{pmatrix} a_+ \\ a_- \end{pmatrix}. \quad (3.40)$$

Then, we can introduce diagonalizing matrix U such that,

$$\begin{pmatrix} a_+ \\ a_- \end{pmatrix} = U \begin{pmatrix} a_x \\ a_y \end{pmatrix}. \quad (3.41)$$

Thus, S_1 becomes,

$$S_1 = (a_x^+, a_y^+) U^+ \begin{pmatrix} 0 & 1 \\ 1 & 0 \end{pmatrix} U \begin{pmatrix} a_x \\ a_y \end{pmatrix}. \quad (3.42)$$

Then, imposing unitarity condition on U such that $UU^+ = U^+U = 1$, and writing S_1 in a_{\pm} basis as

$$S_1 = \begin{pmatrix} 0 & 1 \\ 1 & 0 \end{pmatrix}, \quad (3.43)$$

we demand that U^+SU is a diagonal matrix λ . This leads an eigenvalue problem,

$$U^+SU = \lambda \Rightarrow UU^+SU = U\lambda, \quad (3.44)$$

$$SU = \lambda U \Rightarrow (S - \lambda)U = 0. \quad (3.45)$$

Therefore, we have to determine λ matrix through solving secular equation $\det(S - \lambda) = 0$, or

$$\det \begin{pmatrix} -\lambda & 1 \\ 1 & -\lambda \end{pmatrix} = 0, \quad (3.46)$$

which immediately gives $\lambda = \pm 1$. Using these eigenvalues associated eigenvectors $U_{\pm 1}$ and the U matrix are found to be,

$$U_{-1} = \frac{1}{\sqrt{2}} \begin{pmatrix} 1 \\ -1 \end{pmatrix}, \quad U_1 = \frac{1}{\sqrt{2}} \begin{pmatrix} 1 \\ 1 \end{pmatrix}, \quad (3.47)$$

$$U = \frac{1}{\sqrt{2}} \begin{pmatrix} 1 & 1 \\ 1 & -1 \end{pmatrix}. \quad (3.48)$$

Hence, we conclude that using the transformation

$$a_+ = \frac{a_x + a_y}{\sqrt{2}}, \quad a_- = \frac{a_x - a_y}{\sqrt{2}} \quad (3.49)$$

it is possible to write S_1 in the following diagonal form,

$$S_1 = a_+^+ a_- + a_-^+ a_+ = a_x^+ a_x - a_y^+ a_y. \quad (3.50)$$

Since S_0 and S_3 are already diagonal, then we only need to find another transformation for S_2 only. After a similar analysis, we find,

$$a_+ = i \frac{a_\alpha - a_\beta}{\sqrt{2}}, \quad a_- = \frac{a_\alpha + a_\beta}{\sqrt{2}}. \quad (3.51)$$

In that case, diagonalized S_2 turns out to be,

$$S_1 = i(a_+^\dagger a_- - a_-^\dagger a_+) = a_\beta^\dagger a_\beta - a_\alpha^\dagger a_\alpha. \quad (3.52)$$

Having seen the diagonalization of Stokes operators, we conclude that they are consistent with the operational definition. This makes them valuable for photon counting measurements. Again using polarizers along the path of photons, we can experimentally apply the required transformations since they are merely rotations. However, it is not clear how and why photons respond polarizers. Besides, there is another and even more deep problem related to measurements using photons and quantum light. Eventhough $[S_i, S_0] = 0$, i.e. simultaneous measurements of intensity together with other Stokes operators are possible, simultaneous measurements of other Stokes operators are not possible since,

$$[\hat{S}_i, \hat{S}_j] = -2i\epsilon_{ijk}\hat{S}_k. \quad (3.53)$$

Classically, S_1 can be related to *cosine* of the relative phase between left and right circular polarized components. S_1 can also be related of the *sine* of the same relative phase angle. Since they involve the same phase information, it is rather disturbing that we cannot determine them simultaneously. In fact, this trouble is connected with the famous quantum phase problem, and the lack of well-defined phase operator. Thus, we see that direct second quantization brings not-easily interpretable, and unphysical description of polarization properties of quantum light. In our opinion, one reason that we have these troubles stems from the fact that the electric field given at the very beginning is not valid everywhere. In other words, planewave symmetry is not the natural symmetry of the electromagnetic field. Polarization, as a local property, should be determined within a more general and global framework.

From the set of Stokes operators and their commutation relations, we recognize that they are actually generators of $SU(2)$ algebra. This is the algebra of angular momentum. In Scwinger representation, we notice that $\hat{S}_0 = I$ is the total intensity and $\hat{S}_{1,2,3} \sim \hat{J}_{x,y,z}$ are angular momentum operators. Therefore, this also suggest that electromagnetic field should have a more general symmetry at the very beginning of its evolution, but in the far zone that more global symmetry group is contracted into $SU(2)$ group. It might be possible to recover physical and commuting set of Stokes parameters by a more global construction of Stokes operators. We shall see that, indeed this is possible in some cases.

Finally, another delicate problem is the choice of gauge in the quantization. Above construction uses transversal gauge, and the theory of polarization is gauge dependent. In order to set up a covariant and relativistically consistent theory, it might be necessary also to introduce timelike photons and longitudinal photons and use the Lorentz gauge together with Gupta-Blauler quantization condition. We will be content with addressing this question, in which coherency matrix would be four dimensional, but we will not give an answer here.

3.5 Systematic Approach to Multipole Radiation

In general, we can express the electric and magnetic field components of electromagnetic radiation as a Fourier series, in the form

$$A(r, t) = \sum_{\omega} A(r, \omega) e^{-i\omega t}, \quad (3.54)$$

where A can be E and B as well. Summation could be replaced by an integral for continuous frequency spectrum. In the following analysis, we will treat individual Fourier components of the fields. Applying the assumption of possibility of separating generation region from the propagation region, we write the Maxwell equations for Fourier components, in the propagation region

as source-free Maxwell equations,

$$\vec{\nabla} \times \vec{E} = ik\vec{B}, \quad \vec{\nabla} \cdot \vec{E} = 0, \quad (3.55)$$

$$\vec{\nabla} \times \vec{B} = -ik\vec{E}, \quad \vec{\nabla} \cdot \vec{B} = 0. \quad (3.56)$$

Here $k = \omega/c$. Elimination of E or B by combining the curl equations, we obtain the standard wave equation

$$(\nabla^2 + k^2)\{E, B\} = 0, \quad (3.57)$$

with relations

$$\begin{Bmatrix} E \\ B \end{Bmatrix} = \pm \frac{i}{k} \nabla \times \begin{Bmatrix} B \\ E \end{Bmatrix}. \quad (3.58)$$

Since we are dealing with localized sources, and propagation in free space then we will consider that boundary conditions are spherical. In that case in order to avoid unnecessary complications that can arise by working in a basis refusing the natural spherical symmetry of the problem, we will follow Bouwkamp and Casimir⁶⁷ and write the wave equation as follows,

$$(\nabla^2 + k^2)(r \cdot \{E, B\}) = 0. \quad (3.59)$$

Denoting $r \cdot \{E, B\}$ by $\psi(r, \omega)$, general solution of this wave equation can be written as variable separated form,

$$\psi(r, \omega) = \sum_{jm} f_{jm}(r) Y_{jm}(\theta, \phi) \quad (3.60)$$

Radial functions satisfy an m independent radial equation. After substitution

$$f_j = \frac{1}{\sqrt{r}} u_j, \quad (3.61)$$

it is seen that they indeed satisfy Bessel equation as,

$$\left(\frac{d^2}{dr^2} + \frac{1}{r} \frac{d}{dr} + k^2 - \frac{(j + 1/2)^2}{r^2} \right) u_j(r) = 0. \quad (3.62)$$

Therefore, we write the general solution as,

$$\psi = \sum_{jm} (A_{jm}^1 h_j^1(kr) + A_{jm}^2 h_j^2(kr)) Y_{jm}(\theta, \phi). \quad (3.63)$$

Here, $h_j^{1,2}$ are the spherical Hankel functions,

$$h_j^{1,2}(r) = \sqrt{\frac{\pi}{2r}} (J_{j+1/2}(r) \pm N_{j+1/2}(r)). \quad (3.64)$$

Here J and N are spherical Bessel and Neumann functions. From physical point of view, by considering asymptotics of spherical Hankel functions corresponds the outgoing and incoming waves. In fact, Green function for outgoing spherical waves are proportional to h^1 while Green function of incoming waves are represented in terms of h^2 .

It is convenient and physical to combine radial and angular basis functions into more compact and physical basis functions and define a magnetic multipole of order (j, m) by the condition

$$r \cdot B_{jm}^M = \frac{j(j+1)}{k} g_j(kr) Y_{jm}(\theta, \phi), \quad (3.65)$$

$$r \cdot E_{jm}^M = 0, \quad (3.66)$$

and also an electric multipole of order (j, m) by the condition

$$r \cdot E_{jm}^E = -\frac{j(j+1)}{k} f_j(kr) Y_{jm}(\theta, \phi), \quad (3.67)$$

$$r \cdot B_{jm}^E = 0. \quad (3.68)$$

It is useful to observe that angular momentum nicely enters above definitions. This can be observed by noting that,

$$kr \cdot \{E, B\} = L \cdot \{B, E\}. \quad (3.69)$$

Above relation can be derived through curl relation between E and B . Then, let us consider how can we get E (and B) from the knowledge of $L \cdot E$ and $r \cdot E$. We introduced that,

$$r \cdot E_{jm}^M = 0 \quad (3.70)$$

$$L \cdot E_{jm}^M = j(j+1) Y_{jm} g_j(kr) \quad (3.71)$$

We first note that L acts only on the angular variables, thus radial dependence of E_{jm}^M should be given by $g_j(kr)$. After that, we consider that in general E_{jm}^M should be expressed as an expansion over spherical harmonics. However, if after the action of L , only Y_{jm} is remained, then we conclude that E_{jm}^M should be proportional to LY_{jm} so that $L \cdot LY_{jm} = L^2 Y_{jm} = j(j+1)Y_{jm}$. Moreover, this is consistent with transversality requirement of electric field, of magnetic multipole radiation, namely $r \cdot E^M = 0$, since

$$r \cdot L = 0, \quad (3.72)$$

by definition of L as the orbital angular momentum,

$$L = -i(\mathbf{r} \times \nabla). \quad (3.73)$$

Therefore, our conclusion is that electromagnetic fields of magnetic multipole radiation are specified as

$$\vec{E}_{kjm}^M = g_j(kr) \vec{L} Y_{jm}(\theta, \phi), \quad (3.74)$$

$$\vec{B}_{kjm}^M = -\frac{i}{k} \vec{\nabla} \times \vec{E}_{kjm}^M. \quad (3.75)$$

Due to the fact that electric field is transverse to the propagation direction, or the radius vector r , these fields are also called as transverse electric (TE) multipole fields.

Similarly, for an electric or transverse magnetic multipole of order (j, m) we conclude the following electromagnetic fields are specified,

$$\vec{B}_{kjm}^E = f_j(kr) \vec{L} Y_{jm}(\theta, \phi) \vec{E}_{kjm}^E = \frac{i}{k} \vec{\nabla} \times \vec{B}_{kjm}^E \quad (3.76)$$

Those two sets of multipole fields form a complete set of vector solutions to Maxwell equations in a source-free region. It must be also noted that electric-charge density sources gives rise to electric multipole radiation, and magnetic-moment density sources generates magnetic multipole radiation. Hence, these basis are rather convenient and physical.

Now recalling that we have defined in the very beginning of this chapter vector spherical harmonic X in connection with the angular momentum as

$$\vec{X}_{jm} = \frac{1}{\sqrt{j(j+1)}} \vec{L} Y_{jm}, \quad (3.77)$$

we summarize the complete basis in the following,

$$\vec{E}_{kjm}^M = g_j(kr) \vec{X}_{jm}(\theta, \phi) \quad (3.78)$$

$$\vec{B}_{kjm}^E = f_j(kr) \vec{X}_{jm}(\theta, \phi) \quad (3.79)$$

$$\vec{B}_{kjm}^M = -\frac{i}{k} \vec{\nabla} \times \vec{E}_{kjm}^M \quad (3.80)$$

$$\vec{E}_{kjm}^E = \frac{i}{k} \vec{\nabla} \times \vec{B}_{kjm}^E \quad (3.81)$$

Then, the general solution of the source-free Maxwell equations can be written, for given Fourier components, as

$$\vec{E}_k = \sum_{\Lambda, j, m} a_{\Lambda, k, j, m} \vec{E}_{k, j, m}^{\Lambda}, \quad (3.82)$$

$$\vec{B}_k = \sum_{\Lambda, j, m} a_{\Lambda, k, j, m} \vec{B}_{k, j, m}^{\Lambda}. \quad (3.83)$$

Here $\Lambda = E, M$ distinguishes electric and magnetic multipole components. So far the theory is classical, and the expansion coefficients $a_{k, \Lambda, j, m}$ as well as the coefficients within $f_j(kr)$ and $g_j(kr)$ are determined by the sources and boundary conditions.

From quantum mechanical point of view there is a delicate problem here. Classically it is possible to relate the coefficients $a_{k, \Lambda, j, m}$ directly. However, in quantum mechanics, those coefficients would become photon operators, acting in the Fock number Hilbert space. They are unbounded operators, obey Weyl-Heisenberg algebra. On the other hand, the classical integral relation in terms of the charge density turn out to be strange. Since, this source part connected with a discrete Hilbert space. Interestingly, in Markovian approximation, similar source and photon operator relation can be recovered. In other words, that source and photon operator connection is not as trivial as in the case of source-expansion coefficient connection of classical electrodynamics. The problem is more deep

than it seems and related to the source based quantization problem of quantum electrodynamics.

3.5.1 Multipole fields at different zones of radiation

Above derived general results certainly hold for the intermediate zone, where all terms are of equal importance. At distances close to the source and very far from the source, we can use asymptotics of spherical Hankel functions to find more simple expressions to describe the behavior of the radiation in those zones, and to point out the qualitative differences. Therefore, we begin with recalling the asymptotic forms of spherical functions.

- $r \ll 1, j$

$$j_j(r) \longrightarrow \frac{r^j}{(2j+1)!!} \left(1 - \frac{r^2}{2(2j+3)} + \dots\right) \quad (3.84)$$

$$n_j(r) \longrightarrow -\frac{(2j-1)!!}{r(j+1)} \left(1 - \frac{r^2}{2(1-2j)} + \dots\right) \quad (3.85)$$

- $r \gg j$

$$j_j(r) \longrightarrow \frac{1}{r} \sin\left(r - \frac{j\pi}{2}\right) \quad (3.86)$$

$$n_j(r) \longrightarrow -\frac{1}{r} \cos\left(r - \frac{j\pi}{2}\right) \quad (3.87)$$

Here, $(2j+1)!! = (2j+1)(2j-1)\cdots 3 \cdot 1$. Spherical Bessel $j_j(r)$ and Neumann $n_j(r)$ functions are related to spherical Hankel functions as its real and imaginary parts, respectively.

$$j_j(r) = \sqrt{\frac{\pi}{2r}} J_{j+1/2}(r) \quad (3.88)$$

$$n_j(r) = \sqrt{\frac{\pi}{2r}} N_{j+1/2}(r) \quad (3.89)$$

$$h_j^{1,2}(r) = j_j(r) \pm in_j(r) \quad (3.90)$$

Then for near zone behavior $kr \ll 1$, we obtain

$$B_{jm}^E \longrightarrow -\frac{k}{j} \vec{L} \frac{Y_{jm}}{r^{j+1}}; \quad (3.91)$$

$$E_{jm}^E \longrightarrow -\frac{i}{j} \nabla \times \vec{L} \frac{Y_{jm}}{r^{j+1}} = -\vec{\nabla} \left(\frac{Y_{jm}}{r^{j+1}} \right) \quad (3.92)$$

$$B_{jm}^M \longrightarrow \frac{i}{j} \nabla \times \vec{L} \frac{Y_{jm}}{r^{j+1}} = \vec{\nabla} \left(\frac{Y_{jm}}{r^{j+1}} \right) \quad (3.93)$$

$$E_{jm}^M \longrightarrow -\frac{k}{j} \vec{L} \frac{Y_{jm}}{r^{j+1}}. \quad (3.94)$$

And for the far zone behavior, ignoring the incoming wave part, we get

$$B_{jm}^E \longrightarrow (-i)^{j+1} \frac{e^{ikr}}{kr} \vec{L} Y_{jm} \quad (3.95)$$

$$E_{jm}^E \longrightarrow -(-i)^{j+1} \frac{e^{ikr}}{kr} \vec{n} \times \vec{L} Y_{jm}, \quad (3.96)$$

$$B_{jm}^M \longrightarrow (-i)^{j+1} \frac{e^{ikr}}{kr} \vec{n} \times \vec{L} Y_{jm}, \quad (3.97)$$

$$E_{jm}^M \longrightarrow (-i)^{j+1} \frac{e^{ikr}}{kr} \vec{L} Y_{jm} \quad (3.98)$$

Here, $\vec{n} = \vec{r}/r$ is the unit radial vector. We see that all the fundamental properties of multipole radiation are of those discussed for dipole radiation example. Near to the source, electric field component becomes same with electrostatic solution. Besides, electric field dominates over the magnetic part. Electric field also has a component along the direction of distance vector. In far zone both electric and magnetic field contributes at the same order. Radiation behave like spherical waves. Typical of radiation waves, they are transverse to the radius vector, and falls off r^{-1} .

3.5.2 Separation of longitudinal part: electric, magnetic, and longitudinal vector spherical harmonics

Examining the asymptotic forms of the basis functions for multipole radiation fields, we notice that each involve three significant directions: n , L and $n \times L$. It is natural to ask, whether general compact forms can be written separated explicitly in terms of these directions. It would be nice to see longitudinal part contribution separately from transversal L and $n \times L$ components. In order to achieve this goal, it is convenient to introduce a new set of vector spherical

harmonics,

$$Y_{j,m}^E = \frac{-i}{\sqrt{j(j+1)}}(\vec{n} \times \vec{L})Y_{j,m}(\vec{n}), \quad (3.99)$$

$$Y_{j,m}^M = \frac{1}{\sqrt{j(j+1)}}\vec{L}Y_{j,m}(\vec{n}), \quad (3.100)$$

$$Y_{j,m}^L = \hat{n}Y_{j,m}(\vec{n}). \quad (3.101)$$

Since the basis functions in the form $g_j \vec{X}_{jm}$ are already expressed in terms of $Y_{j,m}^M$, we only need to calculate the compact curl expression $\vec{\nabla} \times f_j \vec{X}_{jm}$ and write it in terms of new set of vector spherical harmonics. Using the differential nature of curl operation and dropping all sub-indices, vector symbols and arguments for the sake of notational simplicity, we get

$$C = \nabla \times fX = (\nabla f) \times X + f\nabla \times X. \quad (3.102)$$

But, since f depends only on r we obtain, after writing X explicitly,

$$C = n \frac{df}{dr} \times \frac{LY}{\sqrt{j(j+1)}} + f \frac{\nabla \times LY}{\sqrt{j(j+1)}}. \quad (3.103)$$

Using the relation,

$$\nabla \times \vec{L} = -ir\nabla^2 - \nabla(1 + r\frac{\partial}{\partial r}), \quad (3.104)$$

C can be written after rearranging the terms,

$$C = \frac{1}{\sqrt{j(j+1)}} \left\{ \frac{df}{dr} n \times LY + f[-inr\nabla^2 + i\nabla(1 + r\frac{\partial}{\partial r})]Y \right\}. \quad (3.105)$$

Since the spherical harmonic doesn't have any spatial dependence, the last term with spatial derivative drops and we get,

$$C = \frac{1}{\sqrt{j(j+1)}} \left[\frac{df}{dr} n \times LY + f(-inr\nabla^2 Y + i\nabla Y) \right]. \quad (3.106)$$

Using the identities,

$$\nabla = \hat{r} \frac{\partial}{\partial r} - \frac{i}{r} \hat{r} \times \vec{L}, \quad (3.107)$$

$$\nabla^2 = \frac{1}{r} \frac{\partial^2}{\partial r^2}(r) - \frac{L^2}{r^2}, \quad (3.108)$$

last two terms in the C expressions are found to be,

$$\nabla Y = -\frac{i}{r} n \times LY, \quad (3.109)$$

$$\nabla^2 Y = -\frac{j(j+1)}{r^2} Y. \quad (3.110)$$

Thus, we have been able to write all the terms involving n and $n \times L$. Note that there is no term with L direction. Resulting expression, using the $Y^{L,E}$ notation, then becomes

$$C = i\left[\left(\frac{df}{dr} + \frac{f}{r}\right)Y^E + \sqrt{j(j+1)}\frac{f}{r}Y^L\right] \quad (3.111)$$

We can also remove explicit spatial dependence and make it implicit. In order to that, we use the following recursion relations of spherical functions,

$$\frac{df_j(kr)}{dr} = \frac{k}{2j+1}(j f_{j-1}(kr) - (1+j)f_{j+1}), \quad (3.112)$$

$$\frac{f_j(kr)}{r} = \frac{k}{2j+1}(f_{j-1} + f_{j+1}). \quad (3.113)$$

Therefore, finally we get the following expression for the electric field basis functions,

$$\vec{E}_{kjm}^E = \frac{-1}{2j+1} \left[u_j(kr) Y_{j,m}^E(\vec{n}) + \sqrt{j(j+1)} v_j(kr) Y_{j,m}^L(\vec{n}) \right], \quad (3.114)$$

$$\vec{E}_{kjm}^M = g_j(kr) \vec{Y}_{jm}^M(\vec{n}). \quad (3.115)$$

Here, we defined two spatial functions u and v as,

$$u_j(kr) = (1+j)f_{j-1} - j f_{j+1}, \quad v_j(kr) = f_{j-1} + f_{j+1}. \quad (3.116)$$

Similar relation can be written down immediately for the magnetic field basis functions. However, our focus will be down on the electric field component of the radiation.

3.5.3 Eigenfunctions of total angular momentum and polarization basis

So far, we have stressed that angular momentum L plays a significant role on determining the direction and hence the polarization properties of the multipole

radiation. In this section we will exploit further the role of angular momentum. Angular momentum, or orbital angular momentum, contributes through the action on spherical harmonics. Let us look at more closely that action. Easiest way is to consider ladder operators L_{\pm} and the z -component of the angular momentum to find its action on spherical harmonic functions. Ladder operators and the z -component appear naturally in a basis defined by

$$e_+ = -\frac{1}{\sqrt{2}}(e_x + ie_y), \quad (3.117)$$

$$e_- = \frac{1}{\sqrt{2}}(e_x - ie_y), \quad (3.118)$$

$$e_0 = e_z. \quad (3.119)$$

We will call this basis as polarization basis. In fact, e_{\pm} represent circular polarization while e_z is linear polarization. For a beam of light propagating along the z direction, e_z also is the direction of propagation. However, we should stress that here we are dealing with spherical waves at far zone and propagation direction in general is the radius vector. In polarization basis, any vector, as well as L can be expressed as

$$L = \sum_{\mu} (-1)^{\mu} e_{-\mu} L_{\mu}. \quad (3.120)$$

Here, polarization components are related to Cartesian components by,

$$L_{\pm 1} = \mp \frac{1}{\sqrt{2}}(L_x \pm iL_y), \quad L_0 = L_z. \quad (3.121)$$

Thus, $L_{\pm 1}$ are proportional to ladder operators L_{\pm} . Therefore, for the action of L on spherical harmonic we have,

$$\hat{L} Y_{jm} = \sum_{\mu} (-1)^{\mu} \vec{e}_{-\mu} \hat{L}_{\mu} Y_{jm}. \quad (3.122)$$

Now, we can recall the result of ladder operations on spherical harmonic, in addition to L_z action,

$$L_{\pm} = L_x \pm iL_y, \quad (3.123)$$

$$L_{\pm} Y_{jm} = \sqrt{j(j+1) - m(m \pm 1)} Y_{j, m \pm 1} \quad (3.124)$$

$$L_z Y_{jm} = m Y_{jm}. \quad (3.125)$$

Then we compare the coefficients on actions of L on Y_{jm} , with the Clebsch-Gordan coefficients obtained by adding 1 unit of spin angular momenta to l unit of orbital angular momenta. In other words, eigenfunctions of total angular momentum

$$J = L + S \quad (3.126)$$

Thus, for a given l we have three values for j namely, $l, l+1, l-1$. Or for a given j we also have three values for l , as $j, j+1, j-1$. Since multipole radiation is classified by j, m it might be better to consider j is specified. Simultaneous eigenfunctions of L^2, S^2, L_z, S_z can be represented by $|l, m_l, 1, \mu \rangle$. We denote the z component quantum numbers by m_l and μ . Since L and S commute, we can also write

$$|l, m_l, 1, \mu \rangle = \chi_\mu Y_{l, m_l} \quad (3.127)$$

Then, we can look for the transformation between the basis $|l, m_l, 1, \mu \rangle$ and the basis $|j, m \rangle$. That new basis $|j, m \rangle$ are the simultaneous eigenkets of J^2, J_z, L^2, S^2 . Completeness relation of the basis vectors $|l, m_l, 1, \mu \rangle$ yields the transformation

$$|j, m \rangle = \sum_{\mu} \chi_\mu Y_{l, m_l} \langle l, m - \mu; 1, \mu | j, m \rangle. \quad (3.128)$$

Note that non-vanishing coefficients of transformation demand $m_l + \mu = m$, and this fact used in above expression for eliminating m_l . The coefficients of the transformation are called as Clebsch-Gordan or Wigner coefficients, and denoted by

$$C(1l\mu, m - \mu | jm) = \langle l, m - \mu; 1, \mu | jm \rangle. \quad (3.129)$$

In our case there are nine coefficients and we introduce a short-hand notation for them as follows,

$$C_{pp'} = C(1lp, m - p | j = l + p', m) = \langle l, m - p; 1, p | j = l + p', m \rangle \quad (3.130)$$

Here, $p = -1, 0, 1$. Then we have the transformation

$$\begin{pmatrix} |j = l + 1, m \rangle \\ |j = l, m \rangle \\ |j = l - 1, m \rangle \end{pmatrix} = \begin{pmatrix} C_{1,1} & C_{1,0} & C_{1,-1} \\ C_{0,1} & C_{0,0} & C_{0,-1} \\ C_{-1,1} & C_{-1,0} & C_{-1,-1} \end{pmatrix} \begin{pmatrix} |l, m - 1; 1, 1 \rangle \\ |l, m; 1, 0 \rangle \\ |l, m + 1, 1, -1 \rangle \end{pmatrix} \quad (3.131)$$

Transformation matrix should be unitary, as can be seen by orthonormality requirement of $|j, m\rangle$ basis. We will illustrate how to determine the elements of the matrix of transformation for C_{0p} . We begin with expressing J^2 in a convenient form,

$$J^2 = L^2 + S^2 + 2L_z S_z + L_- S_+ + L_+ S_- . \quad (3.132)$$

Then, we find its action on $|j = l, m\rangle$ as

$$\begin{aligned} J^2 |j = l, m\rangle &= C_{0,1} J^2 |l, m-1; 11\rangle + C_{00} |l, m; 1, 0\rangle \\ &+ C_{0,-1} |l, m+1, 1, -1\rangle \end{aligned} \quad (3.133)$$

$$\begin{aligned} &= C_{0,1} \{l(l+1) + 2 + 2(m-1)\} \phi_1 \\ &+ \sqrt{2(l+m)(l-m+1)} \phi_2 + C_{00} \{[l(l+1) + 2] \phi_2 \\ &+ \sqrt{2(l+m)(l-m+1)} \phi_1 + \sqrt{2(l-m)(l+m+1)} \phi_3\} \\ &+ C_{0,-1} \{[l(l+1) + 2 - 2(m+1)] \phi_3 \\ &+ \sqrt{2(l-m)(l+m+1)} \phi_2\} \end{aligned} \quad (3.134)$$

$$= l(l+1) |j = l, m\rangle \quad (3.135)$$

Here, $\phi_1 = |l, m-1; 11\rangle$, $\phi_2 = |l, m; 10\rangle$, and $\phi_3 = |l, m+1; 1-1\rangle$. Then grouping and rearranging terms, we equate the coefficients' of ϕ_μ , since they are orthogonal. This gives three coupled linear equations for C_{0p} coefficients. Only two of these equations are independent and they are given by

$$C_{01} = -\frac{2(l+m)(l-m+1)}{2m} C_{00} \quad (3.136)$$

$$C_{0,-1} = \frac{2(l-m)(l+m+1)}{2m} C_{00}. \quad (3.137)$$

Therefore, normalization gives,

$$C_{00} = \frac{m}{\sqrt{l(l+1)}}. \quad (3.138)$$

Positive sign is chosen as a sign convention. Then other coefficients are found to be,

$$C_{0,1} = -\sqrt{\frac{(l+m)(l-m+1)}{2l(l+1)}}, \quad (3.139)$$

$$C_{0,-1} = \sqrt{\frac{(l-m)(l+m+1)}{2l(l+1)}}. \quad (3.140)$$

Other elements of the C matrix can be calculated in a similar manner. We quote the results below,

$$C_{11} = \sqrt{\frac{(l+m)(l+m+1)}{2(l+1)(l+2)}}, \quad (3.141)$$

$$C_{10} = \sqrt{\frac{(l-m+1)(l+m+1)}{(l+1)(l+2)}}, \quad (3.142)$$

$$C_{1,-1} = \sqrt{\frac{(l-m)(l-m+1)}{2(l+1)(l+2)}}, \quad (3.143)$$

$$C_{-1,1} = -\sqrt{\frac{(l-m)(l-m+1)}{2l(2l+1)}}, \quad (3.144)$$

$$C_{-10} = \sqrt{\frac{l^2 - m^2}{l(2l+1)}}, \quad (3.145)$$

$$C_{-1,-1} = -\sqrt{\frac{(l+m)(l+m+1)}{2l(2l+1)}}. \quad (3.146)$$

We can now observe that, it is possible to write action of L on Y_{jm} in terms of Clebsch-Gordan coefficients. For instance, action of L_{+1} can be found as

$$L_{+1}Y_{jm} = -\frac{L_+}{\sqrt{2}}Y_{jm} \quad (3.147)$$

$$= -\sqrt{j(j+1)}\sqrt{\frac{(j-m)(j+m+1)}{2j(j+1)}}Y_{j,m+1} \quad (3.148)$$

$$= -\sqrt{j(j+1)}C(1, -1; j, m+1|jm)Y_{j,m+1}. \quad (3.149)$$

Similarly, we can find

$$L_{-1}Y_{jm} = \frac{L_-}{\sqrt{2}}Y_{jm} \quad (3.150)$$

$$= -\sqrt{j(j+1)}C(1, 1; j, m-1|jm)Y_{j,m-1}; \quad (3.151)$$

$$L_0Y_{jm} = L_zY_{jm} = \sqrt{j(j+1)}C(1, 0; j, m|jm)Y_{j,m}. \quad (3.152)$$

Hence, we finally obtain

$$\hat{L}Y_{jm} = \sum_{\mu} (-1)^{\mu} \vec{e}_{-\mu} \hat{L}_{\mu} Y_{jm} \quad (3.153)$$

$$= \sqrt{j(j+1)} \sum_{\mu} C(1, j, -\mu, m + \mu | jm) \vec{e}_{-\mu}. \quad (3.154)$$

By changing sign of μ , as $\mu \rightarrow -\mu$ we see that the magnetic vector spherical harmonic then can be written as

$$\vec{Y}_{jm}^M = \sum_{\mu} C(1, j, \mu | jm) \vec{e}_{\mu} Y_{j, m-\mu}. \quad (3.155)$$

By comparing this with the transformation

$$|j, m\rangle = \sum_{\mu} C(1, l, \mu, m - \mu | jm) \chi_{\mu} Y_{l, m-\mu}, \quad (3.156)$$

we conclude that spin eigenfunction coincide with the polarization basis and the magnetic vector spherical function is an eigenfunction of the total angular momentum. By a similar analysis, it can be shown that electric and longitudinal spherical harmonics can also be expressed in terms of eigenfunctions of the total angular momentum. We introduce a new notation to denote the eigenfunctions of total angular momentum for a given j .

$$|j = l, m\rangle = Y_{j, j, m} \quad (3.157)$$

$$|j = l + 1, m\rangle = Y_{j, j-1, m} \quad (3.158)$$

$$|j = l - 1, m\rangle = Y_{j, j+1, m}. \quad (3.159)$$

Then, we summarize the relations between vector spherical harmonics and the total angular momentum eigenfunctions.

$$\vec{Y}_{j, m}^M = \vec{Y}_{j, j, m}, \quad (3.160)$$

$$\vec{Y}_{j, m}^E = \frac{1}{\sqrt{2j+1}} (\sqrt{j} \vec{Y}_{j, j+1, m} + \sqrt{j+1} \vec{Y}_{j, j-1, m}), \quad (3.161)$$

$$\vec{Y}_{j, m}^L = -\sqrt{\frac{j+1}{2j+1}} \vec{Y}_{j, j+1, m} + \sqrt{\frac{j}{2j+1}} \vec{Y}_{j, j-1, m}. \quad (3.162)$$

Thus, the multipole electric field basis functions now become,

$$\begin{aligned}\vec{E}_{M,k,j,m} &= g_j(kr)\vec{Y}_{j,j,m}, & (3.163) \\ \vec{E}_{E,k,j,m} &= \frac{1}{\sqrt{(1+2j)}}(\sqrt{j}f_{j+1}(kr)\vec{Y}_{j,j+1,m} - \sqrt{j+1}f_{j-1}(kr)\vec{Y}_{j,j-1,m}). & (3.164)\end{aligned}$$

Since all eigenfunctions of total angular momentum operator are expressed in polarization basis, and basis functions are shown to be linear in them, it is concluded that

$$\Rightarrow \vec{A} = \sum_{\mu} \vec{e}_{\mu} \mathcal{A}_{\mu}, \quad \vec{E}_{\mu} = \sum_{\mu} \vec{e}_{\mu} \mathcal{E}_{\mu}.$$

We should put a word of caution here. Eventhough, we have seen polarization basis coincide with the spin eigenfunctions, we should be careful in interpretation of this result. The reason for that, the spin of photon is an ill-defined and ambiguous concept. In quantum field theory, we can view the spin of a particle as the angular momentum of that particle at rest. However for photons, being particles with vanishing rest mass that definition is problematic. Nevertheless. it is possible to separate the total angular momentum of photon into two parts, one involving spatial parameters, and one involving only intrinsic properties of the field. Then, it is possible to define the spin still as an intrinsic property, with magnitude equal to the minimum value of the angular momentum. Experimentally, minimum value of angular momentum is demonstrated to be unity, and therefore we consider photons as spin 1 particles.

3.6 Local Coherency Matrix and Stokes Operators

Having seen that electric field vector in general have three directions rather than two, it is necessary to generalize the 2×2 coherency matrix to 3×3 . Motivations to define the coherency matrix as $(\vec{e}_{\mu}^* \cdot E(\vec{r}, t))(\vec{e}_{\nu} \cdot E(\vec{r}, t))$ stand the same. By this way, its elements will have all the information on intensities and relative phases

of different polarized components. In contrast to plane wave expansion, spatial dependence is not cancelled, but remained. Then, coherency matrix becomes

$$J = \begin{pmatrix} J_{++} & J_{+-} & J_{+0} \\ J_{-+} & J_{--} & J_{+0} \\ J_{0+} & J_{0-} & J_{00} \end{pmatrix} \quad (3.165)$$

$$= \begin{pmatrix} \mathcal{E}_+ \mathcal{E}_+^* & \mathcal{E}_+ \mathcal{E}_-^* & \mathcal{E}_+ \mathcal{E}_0^* \\ \mathcal{E}_- \mathcal{E}_+^* & \mathcal{E}_- \mathcal{E}_-^* & \mathcal{E}_- \mathcal{E}_0^* \\ \mathcal{E}_0 \mathcal{E}_+^* & \mathcal{E}_0 \mathcal{E}_-^* & \mathcal{E}_0 \mathcal{E}_0^* \end{pmatrix} \quad (3.166)$$

While writing the electric field basis functions of multipole radiation in terms of Y^L, Y^M, Y^E vector spherical harmonics, we noticed that the longitudinal component, Y^L has spatial coefficient v_j , given by

$$v_j = f_{j+1} + f_{j-1}. \quad (3.167)$$

Observing that Y^M and Y^E are always transversal to the radius vector,

$$\vec{n} \cdot \vec{Y}_{jm}^{M,E} = 0, \quad (3.168)$$

we deduce that spatial behavior of electric field is governed by $v_j(kr)$. In other words,

$$(\vec{n} \cdot \vec{E})_j \sim v_j = f_{j+1} + f_{j-1}. \quad (3.169)$$

Using the asymptotic form of spatial functions, for the specific case of outgoing spherical waves, we then conclude that longitudinal part vanishes as r reaches to and increases in the far zone, since

$$f_j \rightarrow (-i)^{1+j} \frac{e^{ikr}}{kr} \implies \vec{e}_0 \cdot \vec{E} = \mathcal{E}_0 \rightarrow 0. \quad (3.170)$$

Thus, the general, spatial (local) coherency matrix is shown to be contracted into and consistent with standard, transversal coherency matrix, as $J_{ij} \rightarrow 0$ for $i = 0$ or $j = 0$ in far zone. This also clearly demonstrates, the standard definition of coherency matrix is not a global one and valid only for far zone.

We have noted that Stokes operators can be associated with generators of $SU(2)$ in the case of standard theory of polarization. This is also useful from physical point of view to make polarization, or helicity and angular momentum connection. We want to emphasize the angular momentum connection as our previous analysis shows how significant quantity it is to determine the direction of electric field. Moreover, it is the only physical quantity involving phase information, since the linear momentum, or energy are not very useful in this context. So bearing these points in mind, we propose that due to the existence of longitudinal mode and spherical symmetry of multipole radiation as well as 3×3 form of generalized, local coherency matrix generators of $SU(3)$ algebra might be realized as generalized, local (spatial) Stokes parameters. Then, we recall the conventional set of generators of $SU(3)$,

$$h_1 = J_{-+} + J_{+-}, \quad h_2 = -i(J_{-+} - J_{+-}), \quad (3.171)$$

$$h_3 = J_{++} - J_{--}, \quad h_4 = J_{0+} + J_{+0}, \quad (3.172)$$

$$h_5 = -i(J_{0+} - J_{+0}), \quad h_6 = J_{0-} + J_{-0}, \quad (3.173)$$

$$h_7 = -i(J_{0-} - J_{-0}), \quad h_8 = \frac{1}{\sqrt{3}}(J_{++} + J_{--} - 2J_{00}). \quad (3.174)$$

In constructing the standard Stokes operators, our purpose was to find intensities and relative phase of two polarized components of transversal field. Since there were three unknowns, three Stokes parameters introduced. Total intensity was also added. Now, since there are three possible directions in general, we need to determine five parameters in order to specify the polarization state. Those five parameters are three intensities of polarized components, and two relative phases. Note that, Eventhough there are three relative phases only two of them are independent, since they all add up to zero,

$$\Delta_{+-} + \Delta_{0+} + \Delta_{-0} = 0. \quad (3.175)$$

Here, Δ_{ij} are the relative phases. Examination of the above set of generators of $SU(3)$, we see that there are two diagonal ones, h_3 and h_8 . Since the total intensity is also diagonal, then we see that for three unknown intensities of

polarized components, we can choose three parameters as h_3, h_8 and the total intensity. Remaining six generators all have relative phase information. Since we have only two unknowns we can group them into two set of generators each involving three generators. While doing that it is useful to group those having the same operator structure. In fact, h_1, h_4 and h_6 looks like to carry information on the *cosine* of relative phases, while h_2, h_5 and h_7 looks like it carries *sine* information of the relative phases. Then, we conclude and propose the following set of Stokes parameters,^{26,27,33-35}

$$S_0 = \text{Tr}(J), \quad (3.176)$$

$$S_1 = h_1 + h_4 + h_6, \quad (3.177)$$

$$S_2 = h_2 + h_5 + h_7, \quad (3.178)$$

$$S_3 = h_3, \quad (3.179)$$

$$S_4 = h_8. \quad (3.180)$$

More explicitly, we can express them as

$$S_0(\vec{r}) = |\mathcal{E}_+(\vec{r})|^2 + |\mathcal{E}_-(\vec{r})|^2 + |\mathcal{E}_0(\vec{r})|^2, \quad (3.181)$$

$$S_1(\vec{r}) = 2\text{Re}[\mathcal{E}_+^*(\vec{r})\mathcal{E}_0(\vec{r}) + \mathcal{E}_0^*(\vec{r})\mathcal{E}_-(\vec{r}) + \mathcal{E}_-^*(\vec{r})\mathcal{E}_+(\vec{r})], \quad (3.182)$$

$$S_2(\vec{r}) = 2\text{Im}[\mathcal{E}_+^*(\vec{r})\mathcal{E}_0(\vec{r}) + \mathcal{E}_0^*(\vec{r})\mathcal{E}_-(\vec{r}) + \mathcal{E}_-^*(\vec{r})\mathcal{E}_+(\vec{r})], \quad (3.183)$$

$$S_3(\vec{r}) = |\mathcal{E}_+(\vec{r})|^2 - |\mathcal{E}_-(\vec{r})|^2, \quad (3.184)$$

$$S_4(\vec{r}) = |\mathcal{E}_+(\vec{r})|^2 + |\mathcal{E}_-(\vec{r})|^2 - 2|\mathcal{E}_0(\vec{r})|^2. \quad (3.185)$$

3.7 Polarization Matrix for Photons

Since the electric field basis of multipole radiation is complete, orthonormal one, as can be seen most easily by its expressions in terms of eigenfunctions of total angular momentum, we can also use them as a basis of expansion for vector potential of multipole radiation. Vector potential plays a key role in quantization. In truth, photons are not quantum particles of electromagnetic field, but technically, they are quanta of massless gauge field A , in other words

they are quantum particles of vector potential. We consider the boundary as a perfectly conducting sphere located at very far distance R from the source located at the center of the sphere. Then that impose the following conditions on spatial field functions,

$$\int_0^R F_j^*(k'r)F_j(kr)r^2 dr = V\delta_{k,k'}, \quad (3.186)$$

$$F_j(kR) = 0, \quad \text{with } F = f, g. \quad (3.187)$$

Note that vanishing field functions at the boundary discretize the k through the zeros of spherical Bessel function. Therefore, in the following we will use summation rather than integration over the k , wave number. We will also fix the gauge as transversal gauge. Thus, positive frequency part of the vector potential can be written as

$$\vec{A}(\vec{r}, t) = \sum_{\Lambda, k, j, m} a_{\Lambda, k, j, m}(t) \vec{E}_{kj m}^{\Lambda}(\vec{r}) \quad (3.188)$$

Then in the transversal gauge, we have for the electric and magnetic fields,

$$\vec{E} = \frac{1}{c} \frac{\partial \vec{A}}{\partial t} \quad (3.189)$$

$$\vec{B} = \vec{\nabla} \times \vec{A}. \quad (3.190)$$

Note that for a free field time dependence of the expansion coefficients are $\exp(-i\omega t)$. However, they can be have different time dependence in the case of interaction. Equation of motion of the vector potential, in other words the source-free wave equation, can be derived from the free field Lagrangian density,

$$\mathcal{L} = \frac{1}{8\pi} \left[\frac{1}{c^2} \left(\frac{\partial \vec{A}}{\partial t} \right)^2 - (\vec{\nabla} \times \vec{A})^2 \right]. \quad (3.191)$$

Quantization prescription also need to know the conjugate momentum of the vector potential. It is given by,

$$\vec{P} = \frac{\partial L}{\partial \frac{\partial \vec{A}}{\partial t}} \quad (3.192)$$

$$= \frac{1}{4\pi c^2} \frac{\partial \vec{A}}{\partial t} \quad (3.193)$$

Then, quantization, in the ideology of Poisson bracket quantization, is accomplished by imposing the condition

$$[\hat{A}_{\Lambda,k,j,m}, \hat{P}_{\Lambda,k,j,m}^\dagger] = i\hbar\delta_{\Lambda',\Lambda}\delta_{k',k}\delta_{j',j}\delta_{m'm} \quad (3.194)$$

Photon picture arises in the occupation number, or Fock number representation. The defining algebra of this representation is the Weyl-Heisenberg algebra, H_4 . It introduces ladder, or creation and annihilation operators a, a^\dagger through the commutation relations

$$[\hat{a}_{\Lambda,k,j,m}, \hat{a}_{\Lambda,k,j,m}^\dagger] = \delta_{\Lambda',\Lambda}\delta_{k',k}\delta_{j',j}\delta_{m'm} \quad (3.195)$$

$$[\hat{a}, \hat{a}] = 0 = [\hat{a}^\dagger, \hat{a}^\dagger]. \quad (3.196)$$

In order to use photon operators then we need to introduce a rescaling factor, which can be interpreted also as the vector potential associated with a single photon, into the expansion of vector potential to make both commutation relations of photons and conjugate generalized coordinates consistent. Then, we get

$$\vec{A}(\vec{r}, t) = \sum_{\Lambda,k,j,m} \mathcal{G}_k \hat{a}_{\Lambda,k,j,m}(t) \vec{E}_{kj m}^\Lambda(\vec{r}), \quad (3.197)$$

where the rescaling factor \mathcal{G}_k is found to be,

$$\mathcal{G}_k = \sqrt{\frac{2\pi\hbar c}{V_k}}. \quad (3.198)$$

Photons introduced in the above formalism are different than the photons of plane wave quantization. For each type of radiation, electrical or magnetic, they are characterized by three quantum numbers, namely wave number k , angular momentum j , and its projection on the quantization axis z as m . They specify physical properties of photons. For example such photon carries energy $\omega = ck$. It has angular momentum $j(j+1)$, with z -component m . Such photons also have parity given by $\pi = (-1)^j$ for $\Lambda = E$, and $\pi = (-1)^{j+1}$ for $\Lambda = M$. It is interesting to note that such description of photons are not compatible with photons of plane wave quantization. In other words, if one basis is chosen for

a particular problem, then the other basis cannot be used since they may not commute. This arises from the following fact. Plane wave representation is for the translational group with linear momentum as its generator. However, due to the spherical symmetry, vector spherical harmonic representation is used. They are for the rotational group with angular momentum as its generator. Angular and linear momentum are non-commuting quantities, therefore we cannot use both representations in a compatible way.

Now, in polarization basis we can express the vector potential as,

$$\vec{A}(r, t) = \sum_{\mu} \vec{e}_{\mu} \hat{A}_{\mu}, \quad (3.199)$$

where,

$$\hat{A}_{\mu}(\vec{r}, t) = \sum_{\Lambda, k, j, m} \mathcal{G}_k \hat{a}_{\Lambda, k, j, m}(t) [\vec{E}_{kjm}^{\Lambda}(\vec{r})]_{\mu}. \quad (3.200)$$

Using $\vec{E} = -\partial \vec{A} / \partial ct$, and ∂t , and

$$\frac{\partial \hat{a}_{\Lambda k j m}}{\partial t} = -ick \hat{a}_{\Lambda k j m}, \quad (3.201)$$

components of electric field in polarization basis are found to be,

$$\hat{\mathcal{E}}_{\mu}(\vec{r}, t) = \sum_{\Lambda, k, j, m} ik \mathcal{G}_k \hat{a}_{\Lambda, k, j, m}(t) [\vec{E}_{kjm}^{\Lambda}(\vec{r})]_{\mu}. \quad (3.202)$$

Commutation relation among the photon operators bring a scalar, in other words commutation of these polarized field component operators doesn't include any operator. Hence we write,

$$[\mathcal{E}_{\mu}(\vec{r}), \mathcal{E}_{\mu'}^{\dagger}(\vec{r}')] = M_{\mu, \mu'}(\vec{r}, \vec{r}') \quad (3.203)$$

Note that, since the right hand side is not unity, we cannot consider them as photon operators with given polarization, at a given point. In order to define quanta of field in the polarization basis, with a given polarization at a given point, we need to go for occupation number representation. Here, the matrix $M(\vec{r}, \vec{r}') = M(\vec{r})$ is 3×3 Hermitian matrix, it can be diagonalized into a real,

diagonal 3×3 matrix $D(\vec{r})$ by a unitary matrix $U(\vec{r})$ such that $UMU^\dagger \equiv D(\vec{r})$. This unitary matrix can be introduced by photon counters, and polarizers in an operational way. In a similar way, we obtained rescaling of vector potential for photon representation, we can also see this transformation as a rescaling operation to receive Weyl-Heisenberg algebra at any distance. In other words, we introduce new operators, $\hat{p}_\mu(\vec{r}, t)$ instead of operators \mathcal{E}_μ such that,

$$[\hat{p}_\mu(\vec{r}, t), \hat{p}_{\mu'}] = \delta_{\mu, \mu'}. \quad (3.204)$$

Then, required transformation is find to be,

$$\hat{p}_\mu(\vec{r}, t) \equiv \frac{1}{\sqrt{D_\mu(\vec{r})}} \sum_{\mu'} U_{\mu\mu'}(\vec{r}) \hat{\mathcal{E}}_{\mu'}(\vec{r}) \quad (3.205)$$

These operators describe quanta of the polarization components of the electric field. Even though, they obey the H_4 -algebra, they don't necessarily coincide, in general, with photons of the vector potential. However, they do so in certain special cases, as we shall see and discuss in the next section.

3.8 Radiation along the z -Direction

In this section, we explore more closely a common example. We consider that a detector is placed somewhere along the z axis. In this case, results are greatly simplified, as we can ignore the angular complications. Since now $\vec{n} = \vec{e}_0$, and $\theta = \phi = 0$, we can use the identity,

$$Y_{j,m}(0,0) = \sqrt{\frac{2j+1}{4\pi}} \delta_{m0}. \quad (3.206)$$

Note that this identity is also valid for $\phi \neq 0$. Then, by straightforward application of the orbital angular momentum,

$$\vec{L} = \vec{e}_0 L_z + \vec{e}_- \frac{1}{\sqrt{2}} L_+ - \vec{e}_+ \frac{1}{\sqrt{2}} L_-, \quad (3.207)$$

yields,

$$\vec{Y}_{jm}^M(0,0) = \frac{1}{\sqrt{j(j+1)}} \vec{L} Y_{jm}(0,0) = \sqrt{\frac{2j+1}{8\pi}} (\vec{e}_- \delta_{m,-1} - \vec{e}_+ \delta_{m,+1}), \quad (3.208)$$

$$\begin{aligned}
\vec{Y}_{jm}^E(0,0) &= \frac{-i}{\sqrt{j(j+1)}} \vec{e}_0 \times \vec{L} Y_{jm}(0,0) = -\sqrt{\frac{2j+1}{8\pi}} (\vec{e}_- \delta_{m,-1} + \vec{e}_+ \delta_{m,1}) \\
\vec{Y}_{jm}^L(0,0) &= \vec{e}_0 \sqrt{\frac{2j+1}{4\pi}} \delta_{m,0}.
\end{aligned} \tag{3.210}$$

Therefore, we conclude that for any given 2^j -pole radiation, right and left circular polarized components propagating along the z direction always consists of photons with z -component of their angular momentum is $m = \pm 1$. This is the concept of helicity, and explains why and how far we can use helicity and polarization in common grounds. Longitudinally polarized radiation along the z direction consists of photons with vanishing z -component of angular momentum, $m = 0$. We see that, considering a given charge distribution, so that $\Lambda = E$, and presuming monochromatic radiation with a well defined, fixed angular momentum then we get 1 – 1 correspondence as $\hat{p}_\mu = \hat{a}_{Ekj\mu}$. In that case, and for dipole, $E1$ radiation, then generalized Stokes operators are expressed in the following form,

$$\begin{aligned}
S_0 &= \sum_{m=-1}^{+1} a_m^\dagger a_m \\
S_1 &= \frac{1}{2} (a_+^\dagger a_0 + a_0^\dagger a_- + a_-^\dagger a_+ + h.c.) \\
S_2 &= \frac{1}{2i} (a_+^\dagger a_0 + a_0^\dagger a_- + a_-^\dagger a_+ - h.c.) \\
S_3 &= \sum_{m=-1}^{+1} m a_m^\dagger a_m \\
S_4 &= a_+^\dagger a_+ + a_-^\dagger a_- - 2a_0^\dagger a_0
\end{aligned} \tag{3.211}$$

Here, coefficients of S_1 and S_2 are chosen for convenience.

$$[S_0, S_1] = [S_0, S_2] = [S_1, S_2] = 0$$

Thus, simultaneous measurements are possible.

3.9 Dipole radiation

When multipole radiation is specified to be generated by a charge distribution, and $j = 1$, it is called as electric dipole radiation, or $E1$ radiation. Since higher order multipole radiations are much weaker, and more complicated, $E1$ radiation is popular both in theoretical and experimental optical studies. Here, we will examine this radiation from the point of view of above developed ideology.

3.9.1 Quantum fluctuations of the generalized Stokes parameters

Quantum fluctuations of an operator S are determined by its variance, defined by

$$V(S) = \langle S^2 \rangle - \langle S \rangle^2 \quad (3.212)$$

As a particular case, both circularly polarized components of $E1$ radiation are in the coherent states with one and the same intensity, and longitudinal component is in vacuum state can be considered. This is typical, but simplified by choosing equal intensities, situation for far zone radiation. In this case, expectation values of Stokes operators lead to

$$\begin{aligned} \langle S_1 \rangle &= |\alpha|^2 \cos \Delta_{+-}, \\ \langle S_2 \rangle &= |\alpha|^2 \sin \Delta_{+-}, \\ \langle S_0 \rangle &= 2|\alpha|^2, \quad \langle S_3 \rangle = 0 \end{aligned} \quad (3.213)$$

where α_{\pm} is the parameter of corresponding coherent state, $|\alpha_{\pm}| \equiv |\alpha|$, and $\Delta_{+-} \equiv \arg \alpha_+ - \arg \alpha_-$. We see that generalized Stokes operators give the same results with standard Stokes operators, and no difference can be seen as long as longitudinal component is in vacuum. On the other hand, if we calculate the variances of generalized Stokes operators, we see that they are drastically different from the variance of standard Stokes operators, even when the longitudinal component vanishes. This is fully a quantum effect and stems from the fact that even in vacuum longitudinal mode contributes as vacuum fluctuations due to the noncommutativity in Weyl-Heisenberg algebra. For instance, fluctuations of S_1 is calculated to be

$$V(S_1) = |\alpha|^2 \left(1 + \frac{1}{2} \cos \Delta_{+-} \right). \quad (3.214)$$

For standard S_1 this is found to be $|\alpha|^2/2$. Thus, the quantum fluctuations of S_1 are much stronger than that for the standard one. Moreover, they are qualitatively different because of the dependence on relative phase Δ_{+-} . Similar result can be obtained for S_2 as well. Let us stress that the fluctuations of the total

intensities of both the generalized and the standard Stokes operators have the same magnitude in the case of the vacuum longitudinal field under consideration. Thus, it is shown that the contribution of the longitudinal component of dipole radiation into the quantum fluctuations of the Stokes parameters is important even if this component is taken in the vacuum state when it does not contribute into the Stokes parameters per se.

As polarization is a phase dependent quantity, it is possible to determine the fluctuations in different ways developed for quantum phase problem. Let us compare our results with those obtained within the Pegg-Barnett approach (PBA)²² which has received a lot of attention during last ten years (see, for a recent review Ref.^{68,25}) and has led to many important results. We use here the form of PBA has been considered in Ref.⁶⁹ Then, the phase distribution over the phases of two circularly polarized modes is determined as follows

$$P_\psi = |\langle \phi_+, \phi_- | \psi \rangle|^2 \quad (3.215)$$

where $|\phi_+, \phi_- \rangle$ is the Susskind-Glogower phase state and $|\psi \rangle$ is the state of the radiation field. Similar to above consideration, we suppose that $|\psi \rangle = |\alpha_+ \rangle |0_0 \rangle |\alpha_- \rangle$. Since our formalism is focused on the phase difference rather than individual phase we need to use the distribution function for the relative phase $\phi = \phi_+ - \phi_-$. Referring the procedure suggested in^{25,69} to cast the range of ϕ into 2π range from 4π range, we take

$$P_{2\pi} = \sum_{n=0}^{\infty} |\langle \phi^{(n)} | \psi \rangle|^2, \quad (3.216)$$

$$|\phi^{(n)} \rangle = \frac{1}{\sqrt{2\pi}} \sum_{n_+=0}^n e^{i\phi n_+} |n_+, 0, n - n_+ \rangle. \quad (3.217)$$

Using this distribution function, one can calculate the mean value of any function $F(\phi)$ of the relative phase as follows

$$\langle F(\phi) \rangle = \int_{-\pi}^{\pi} d\phi P_{2\pi}(\phi) F(\phi). \quad (3.218)$$

Then

$$\langle \cos \hat{\phi}_{PB} \rangle = e^{-(I_+ + I_-)} \sum_{n_{\pm}=0}^{\infty} \frac{I_+^{n_+} I_-^{n_-}}{n_+! n_-!} \frac{\text{Re}(\alpha_+ \alpha_-^*)}{\sqrt{(n_+ + 1)(n_- + 1)}} \quad (3.219)$$

$$\langle \cos^2 \hat{\phi}_{PB} \rangle = \frac{1}{2} + \frac{e^{-(I_+ + I_-)}}{2} \sum_{n_{\pm}=0}^{\infty} \frac{I_+^{n_+} I_-^{n_-}}{n_+! n_-!} \frac{Re(\alpha_+ \alpha_-^*)}{\sqrt{(n_+ + 2)(n_+ + 1)(n_- + 2)(n_- + 1)}}. \quad (3.220)$$

Here, $I_m = |\alpha_m|^2$. To clarify the difference between generalized Stokes operators result and these results obtained within PBA, let us represent generalized Stokes operator results presented above, in the following forms

$$\langle S_1 \rangle = \sqrt{I_+ I_-} \cos \Delta_{+-} \quad (3.221)$$

$$= Re(\alpha_+ \alpha_-^*) e^{-(I_+ + I_-)} \sum_{n_{\pm}=0}^{\infty} \frac{I_+^{n_+} I_-^{n_-}}{n_+! n_-!} \quad (3.222)$$

$$\langle S_1^2 \rangle = \frac{1}{2} (\sqrt{I_+ I_-} \cos \Delta_{+-} + I_+ I_- \cos 2\Delta_{+-} + I_+ + I_- + I_+ I_-) \quad (3.223)$$

$$= \frac{1}{2} (\sqrt{I_+ I_-} \cos \Delta_{+-} + 2I_+ I_- \cos^2 \Delta_{+-} + I_+ + I_-) \quad (3.224)$$

$$(3.225)$$

In order to make S_1 similar to *cosine* we need to normalize it by dividing $\sqrt{I_+ I_-}$. After that, we see that Pegg-Barnett *cosine* and normalized S_1 behave qualitatively similarly. If we also normalize S_1^2 say by $\langle S_1^2 + S_2^2 \rangle = 1$, we still cannot obtain qualitatively similar behaving S_1^2 and Pegg-Barnett $\cos^2 \phi_{PB}$. Such a normalization would yield a normalization factor,

$$K = [I_+ + I_- + I_+ I_-]^{-1/2}. \quad (3.226)$$

Then S_1^2 would be,

$$\langle S_1^2 \rangle = \frac{1}{2} + K^2 \frac{1}{2} Re(\alpha_+ \alpha_-^*) e^{-(I_+ + I_-)} \sum_{n_{\pm}=0}^{\infty} \frac{I_+^{n_+} I_-^{n_-}}{n_+! n_-!} + K^2 I_+ I_- \cos 2\Delta_{+-}. \quad (3.227)$$

We see that eventhough the first two terms in normalized S_1^2 behaves qualitatively similar to Pegg-Barnett $\cos^2 \phi_{PB}$, the last term cannot be compensated. In fact, the last terms results from the vacuum contribution of the longitudinally polarized mode, and describes a qualitative quantum effect, which is valid even in far zone.

In Fig.3.4, we demonstrate that effect. It is strongest when one of the transversal, circularly polarized mode is a quantum light, in other words with intensity less than unity.

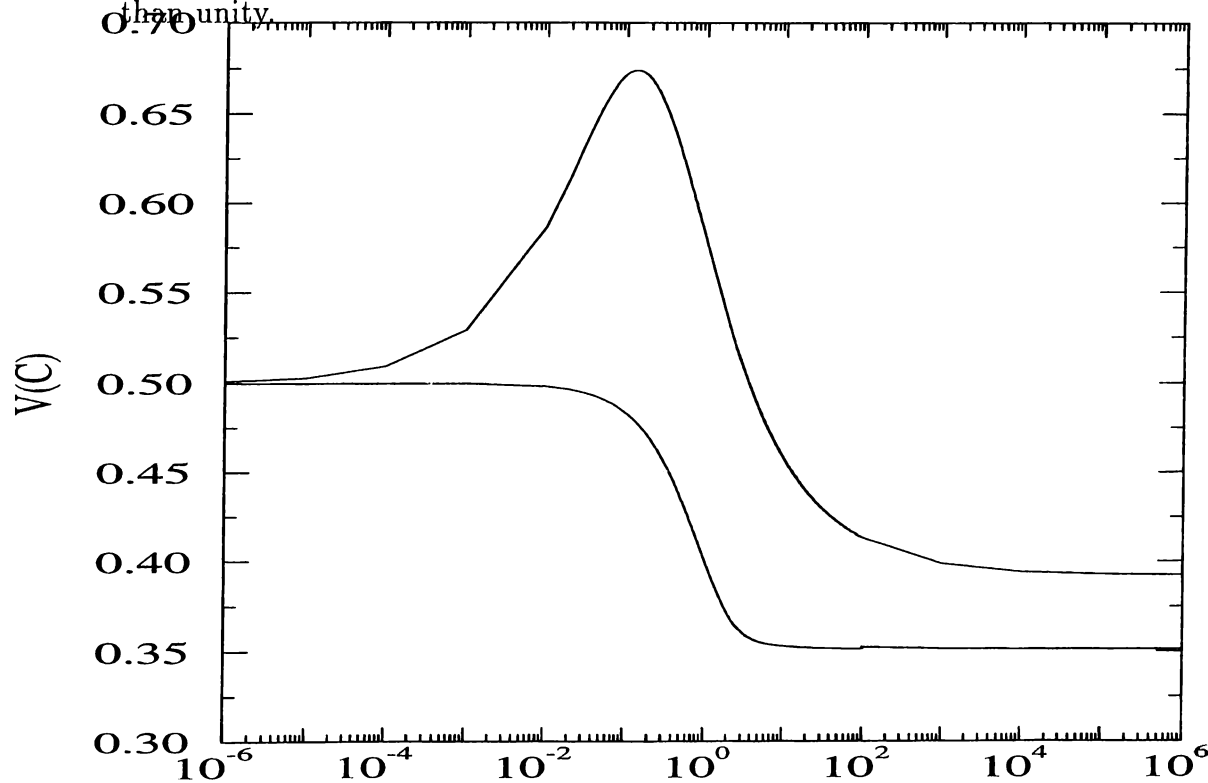


Figure 3.4: Variance of normalized S_1 compared with Pegg-Barnett approach. Lower curve is of the Pegg-Barnett cosine, the upper is of the C_R operator. Both curves are drawn for $\delta = 0$ and $I_+ = 0.275$.

3.9.2 Source-field communication in $E1$ -radiation

Let us consider the Jaynes-Cummings model (here-after JCM) describing the electric dipole transition. The model Hamiltonian has the form

$$H = \sum_{m=-1}^{+1} [\omega a_m^+ a_m + \omega_0 R_{mm} + ig(R_{mG} a_m - a_m^+ R_{Gm})], \quad (3.228)$$

$$g = D \sqrt{\frac{c^4 \omega_0^2}{\hbar V \omega_3}}. \quad (3.229)$$

Here the atomic operators $R_{\alpha\beta} \equiv ||\alpha\rangle\langle\beta||$, the states $||m\rangle \equiv |j = 1; m\rangle$, $m = 0, \pm 1$, correspond to the triple degenerated excited state, $||G\rangle \equiv |j' = 0; 0\rangle$

describes the atomic ground state, the operators a_m^+, a_m describe the electric dipole photons, ω is the radiation frequency, ω_0 is the transition frequency, g is the coupling constant depending on the effective dipole factor D and the volume of quantization V . Let us note that similar Hamiltonians have been considered in many problems of quantum optics and solid state physics (see²⁸ and references therein).

In the basis of the atomic states $||m\rangle$, the representation of the generators of the $SU(2)$ algebra describing the angular momentum \vec{J} , has the form

$$J_z = R_{++} - R_{--}, \quad J_+ = \sqrt{2}(R_{+0} + R_{0-}), \quad (3.230)$$

$$J_- = \sqrt{2}(R_{0+} + R_{-0}) \quad (3.231)$$

with the standard commutation relations

$$[J_z, J_{\pm}] = \pm J_{\pm}, \quad [J_+, J_-] = 2J_z \quad (3.232)$$

and the Casimir operator

$$(\vec{J})^2 = 2 \sum_m R_{mm} \equiv 2 \times \mathbf{1} \quad (3.233)$$

where $\mathbf{1}$ is the unit operator. Then, the polar decomposition of (2) is provided by the exponential of the phase operator⁷¹

$$E = R_{+0} + R_{0-} + e^{i\psi} R_{-+}, \quad EE^+ = \mathbf{1}, \quad E^3 = e^{i\psi} \mathbf{1} \quad (3.234)$$

and the radial operator $J_r = \sqrt{2}(\mathbf{1} - R_{--})$ such that $J_+ = J_r E$. Here ψ is an arbitrary real parameter. Clearly E is similar to the Coxeter operator.⁷² Then, the Hermitian sine and cosine of the atomic phase operators are

$$S = \frac{E - E^+}{2i}, \quad C = \frac{E + E^+}{2} \quad (3.235)$$

One can see that $[S, C] = 0$ and $S^2 + C^2 = \mathbf{1}$. Using the transformation

$$||\varphi_m\rangle = \sum_{n=-1}^{+1} \frac{e^{-2imn\pi}}{\sqrt{3}} ||m\rangle, \quad \varphi_m = \frac{2m\pi - \psi}{3}$$

one can introduce a new basis $||\varphi_m\rangle$, $m = 0, \pm 1$, such that $E||\varphi_m\rangle = e^{i\varphi_m}||\varphi_m\rangle$. Then, the Hermitian atomic phase operator ϕ clearly is

$$\phi = \sum_{m=-1}^{+1} \varphi_m ||\varphi_m\rangle \langle \varphi_m|| = -\frac{\psi}{3} \mathbf{1} - \frac{2i\pi}{3\sqrt{3}} (e^{-i\psi/3} E - e^{i\psi/3} E^+). \quad (3.236)$$

It describes the azimuthal phase of the angular momentum \vec{J} . One can see that $S = \sin \phi$ and $C = \cos \phi$. The representation of the $SU(2)$ algebra in the basis $||\varphi_m\rangle$ is of the form

$$\begin{aligned} \Phi_z &= \sum_{m=-1}^{+1} m ||\varphi_m\rangle \langle \varphi_m|| = -2(S \cos \frac{\psi}{3} + C \sin \frac{\psi}{3}), \\ \Phi_+ &= \sum_{m=-1}^{+1} \sqrt{2 - m(m+1)} ||\varphi_{m+1}\rangle \langle \varphi_m||, \quad \Phi_- = (\Phi_+)^+ \end{aligned} \quad (3.237)$$

where the operators Φ obey the commutation relations (3). Clearly the representation (7) is dual to (2).⁷¹ It follows from (7) that $\Phi_z = -2 \sin(\phi + \mathbf{1}\psi/3)$. The polar decomposition in the dual representation of $SU(2)$ is determined by corresponding unitary exponential operator

$$\epsilon = ||\varphi_+\rangle \langle \varphi_0|| + ||\varphi_0\rangle \langle \varphi_-\rangle + e^{i\chi} ||\varphi_-\rangle \langle \varphi_+||, \quad \epsilon \epsilon^+ = \mathbf{1}, \quad \epsilon^3 = e^{i\chi} \mathbf{1} \quad (3.238)$$

and the radial operator $\Phi_r = \sum_m \sqrt{2 - m(m+1)} ||\varphi_{m+1}\rangle \langle \varphi_{m+1}||$. Here χ is an additional real parameter. Since we are primarily interested in the qualitative results, we may assume that $\chi = 0$. It enables us to fairly simplify the analysis with no loss in generality. Then

$$\epsilon = e^{2i\pi/3} R_{++} + R_{00} + e^{-2i\pi/3} R_{--}.$$

Thus, in addition to S and C , one can introduce the dual sine, cosine and the phase operators as follows

$$S_\Phi = \frac{\epsilon - \epsilon^+}{2i} = \frac{\sqrt{3}}{2} (R_{++} - R_{--}), \quad (3.239)$$

$$C_\Phi = \frac{\epsilon + \epsilon^+}{2} = R_{00} - \frac{1}{2} (R_{++} + R_{--}), \quad (3.240)$$

$$\phi_\Phi = \frac{2\pi}{3} (R_{++} - R_{--}) = \frac{4\pi}{3\sqrt{3}} S_\Phi \quad (3.241)$$

Thus, the quantum phase properties of the atomic angular momentum \vec{J} are completely determined by the set of nine Hermitian operators $\mathbf{1}, J_z, S, C, \phi, \Phi_z, S_\Phi, C_\Phi, \phi_\Phi$. Among them, only five are independent at any real ψ . Therefore, below we put $\psi = 0$ for simplicity and turn our attention to the operators $\mathbf{1}, S, C, S_\Phi, C_\Phi$. In that case, replacing atomic operators with field operators, we obtain

$$S_0 = \sum_{m=-1}^{+1} a_m^\dagger a_m \equiv \hat{n} \quad (3.242)$$

$$S_1 = \frac{1}{2}(a_+^\dagger a_0 + a_0^\dagger a_- + a_-^\dagger a_+ + h.c.) \quad (3.243)$$

$$S_2 = \frac{1}{2i}(a_+^\dagger a_0 + a_0^\dagger a_- + a_-^\dagger a_+ - h.c.) \quad (3.244)$$

$$S_3 = \frac{\sqrt{3}}{2} \sum_{m=-1}^{+1} m a_m^\dagger a_m \quad (3.245)$$

$$S_4 = a_0^\dagger a_0 - \frac{1}{2}(a_+^\dagger a_+ + a_-^\dagger a_-) \quad (3.246)$$

Therefore, we note that these set of Stokes operators are coincide, apart from not important coefficients and signs, with the previously proposed generalized Stokes operators. Thus, we conclude that proposed Stokes operators reflect the source symmetry, and demonstrates how the polarization information naturally transferred from source to light field. The mechanism behind that polarization information transfer is seen to be the conservation of angular momentum. In order to see that better, let us recall the field angular momentum operators,

$$M_z = \sum_{m=-1}^{+1} m a_m^\dagger a_m, \quad (3.247)$$

$$M_+ = \sqrt{2}(a_+^\dagger a_0 + a_0^\dagger a_-), \quad (3.248)$$

$$M_- = \sqrt{2}(a_0^\dagger a_+ + a_-^\dagger a_0). \quad (3.249)$$

These are the generators for the the sub-algebra $SU(2)$ in the Weyl-Heisenberg algebra corresponding to the $E1$ photons. It is clear that $[J_z + M_z, H] = [J_\pm + M_\pm, H] = 0$. However, there is a principal difference between the $SU(2)$ algebra (2) and the sub-algebra (6). Precisely, unlike the eq. (3), the Casimir

operator \vec{M}^2 of (6) cannot be defined as a C -number in the whole Hilbert space describing the radiation field. Therefore, the polar decomposition of the field angular momentum (6) cannot be determined. At the same time, the conservation of the total angular momentum $[\vec{J} + \vec{M}, H] = 0$ permits us to choose the field operator constructions which complement the atomic cosine and sine operators with respect to the integrals of motion. These constructions clearly are

$$\begin{aligned} C_R &= \frac{1}{2} \left(\frac{M_+ + M_-}{\sqrt{2}} + e^{i\psi} a_-^\dagger a_+ + e^{-i\psi} a_+^\dagger a_- \right), \\ S_R &= \frac{1}{2i} \left(\frac{M_+ - M_-}{\sqrt{2}} + e^{i\psi} a_-^\dagger a_+ - e^{-i\psi} a_+^\dagger a_- \right) \end{aligned} \quad (3.250)$$

By choosing $\psi = 0$, they are S_1, S_2 . In other words, the form of Stokes operators is also suggested by the source and this answers why and how the convenient set of generators of $SU(3)$ is used to construct Stokes operators in our previous discussions.

We will now examine the dynamics of the problem more closely. As an ordinary JCM, the model $E1$ Hamiltonian can be solved exactly. Note that this model is also called as color model, due to the existence of degenerate m -levels. Consider first the case when the atom is prepared initially in a linear mixture of two excited states $p|+\rangle + q|-\rangle$, where p, q are complex parameters such that $|p|^2 + |q|^2 = 1$. The field is initially in the vacuum state. Then the radiation of two circularly polarized modes occur. As can be seen from the definitions of S_1, S_2 , the terms with M_\pm do not contribute into the average S_1 and S_2 in this case. In the following, we will call S_1, S_2 as C_R, S_R , radiation cosine and radiation sine, respectively. While doing that we will also introduce normalization constants K_c, K_s to enforce *cosine* and *sine* limits on S_1, S_2 . The time-dependent averages of C_R, S_R are

$$\langle C_R \rangle_t = \frac{K_c}{2} \langle e^{i\psi} a_-^\dagger a_+ + e^{-i\psi} a_+^\dagger a_- \rangle_t, \quad (3.251)$$

$$\langle S_R \rangle_t = \frac{1}{2i} \langle e^{i\psi} a_-^\dagger a_+ - e^{-i\psi} a_+^\dagger a_- \rangle_t. \quad (3.252)$$

These averages formally coincide with the time-dependent standard Stokes parameters describing the cosine and sine of the classical phase difference between

two circularly polarized modes shifted by an arbitrary reference phase ψ . The explicit forms of the averages (8) clearly are

$$\langle C_R \rangle_t = |pq| \sin^2 gt \cos(\delta_{+-} + \psi), \quad (3.253)$$

$$\langle S_R \rangle_t = |pq| \sin^2 gt \sin(\delta_{+-} + \psi). \quad (3.254)$$

Here $\delta_{+-} \equiv \arg p - \arg q$ and we put $\omega = \omega_0$ for simplicity. Parameters $K_c, K_s = 1$ due to the conservation laws

$$\langle C_A + C_R \rangle_t = |pq| \cos(\delta_{+-} + \psi), \quad (3.255)$$

$$\langle S_A + S_R \rangle_t = |pq| \sin(\delta_{+-} + \psi). \quad (3.256)$$

Since there is no loss in generality in choosing $\psi = 0$, one can see that the evolution of the Stokes parameters is completely determined by the parameters of the atomic sub-system p, q and g . And for the variances, we find

$$V_t(C_R) = \sin^2 gt \left[\frac{1}{2}(1 + |pq| \cos \delta_{+-}) - |pq|^2 \cos^2(\delta_{+-} + \psi) \cdot \sin^2 gt \right] \quad (3.257)$$

$$V_t(S_R) = \sin^2 gt \left[\frac{1}{2}(1 - |pq| \cos \delta_{+-}) - |pq|^2 \sin^2(\delta_{+-} + \psi) \cdot \sin^2 gt \right] \quad (3.258)$$

Let us stress here that $\forall t \quad \langle C_A^2 + S_A^2 \rangle_t = 1$ while $\langle C_R^2 + S_R^2 \rangle_t = \sin^2 gt$.

The above consideration can be easily generalized to the case of the initial state $(p||+) + q||-) + r||0\rangle)|0, 0, 0\rangle$ with $|p|^2 + |q|^2 + |r|^2 = 1$. For example, for averages we get

$$\langle C_R \rangle_t = [|pr| \cos \delta_{+0} + |qr| \cos \delta_{-0} + |pq| \cos(\delta_{+-} + \psi)] \cdot \sin^2 gt, \quad (3.259)$$

$$\langle S_R \rangle_t = [|pr| \sin \delta_{+0} + |qr| \sin \delta_{-0} + |pq| \sin(\delta_{+-} + \psi)] \cdot \sin^2 gt. \quad (3.260)$$

Here $\delta_{+0} \equiv \arg p - \arg r$ and $\delta_{-0} \equiv \arg q - \arg r$, and evolution of the cosine and sine is again completely determined by the atomic source parameters.

Above, we examined spontaneous emission problem. Now let us consider the following case of resonance fluorescence. Suppose for initial conditions, that the field consists of two circularly polarized components in coherent state each, and longitudinal mode is in vacuum state. The atom is supposed to be initially in

the ground state. Then, the condition $\langle C_R^2 + S_R^2 \rangle = 1$ gives $K_c = K_s = K = (\bar{n} + \bar{n}_+ \bar{n}_-)^{-1/2}$, where $\bar{n}_\pm \equiv |\alpha_\pm|^2$ denotes the initial mean number of photons with corresponding helicity and $\bar{n} = \bar{n}_+ + \bar{n}_-$. Then, the time-dependent wave function of the system has the form

$$|\Psi(t)\rangle = \sum_{n_+, n_-} P(n_+, n_-) [\cos(g\sqrt{n}t) |G\rangle + (\alpha_+ |+\rangle + \alpha_- |-\rangle) \xi(n_+, n_-) |n_+, 0, n_-\rangle], \quad (3.261)$$

where $n = n_+ + n_-$ and

$$\xi(n_+, n_-) = \frac{\sin(gt\sqrt{n+1})}{\sqrt{n+1}} e^{-i(n+1)\omega t}. \quad (3.262)$$

It is seen that the parameters p, q , describing as above the population of the excited sub-levels, satisfy the conditions $p \sim \exp(i\delta_+)$, $q \sim \exp(i\delta_-)$, $\delta_m \equiv \arg \alpha_m$ so that the induced atomic phase difference is $\delta_{+-} = \delta_+ - \delta_-$. The averaging with the function (10) then gives

$$\langle C_R \rangle_t = K \frac{\sqrt{\bar{n}_+ \bar{n}_-}}{\bar{n}} \langle n \rangle_t \cos(\delta_{+-} + \psi), \quad (3.263)$$

$$\langle S_R \rangle_t = K \frac{\sqrt{\bar{n}_+ \bar{n}_-}}{\bar{n}} \langle n \rangle_t \sin(\delta_{+-} + \psi), \quad (3.264)$$

$$V_t(C_R) = \frac{\langle n \rangle_t}{\bar{n}} [V_{t=0}(C_R) + \beta_c Q], \quad (3.265)$$

$$V_t(S_R) = \frac{\langle n \rangle_t}{\bar{n}} [V_{t=0}(S_R) + \beta_s Q]. \quad (3.266)$$

Here,

$$V_{t=0}(C_R) = \frac{K^2}{2} (\bar{n} + \sqrt{\bar{n}_- \bar{n}_+} \cos \delta_{+-}), \quad (3.267)$$

$$V_{t=0}(S_R) = \frac{K^2}{2} (\bar{n} - \sqrt{\bar{n}_- \bar{n}_+} \cos \delta_{+-}), \quad (3.268)$$

$$\beta_c = K^2 \frac{\bar{n}_+ \bar{n}_-}{\bar{n}} \cos^2(\delta_{+-} + \psi), \quad (3.269)$$

$$\beta_s = K^2 \frac{\bar{n}_+ \bar{n}_-}{\bar{n}} \sin^2(\delta_{+-} + \psi), \quad (3.270)$$

Q is the Mandel's factor determined for the total intensity $Q = (\langle n^2 \rangle_t - \langle n \rangle_t^2 - \langle n \rangle_t) / \langle n \rangle_t$, and

$$\langle n \rangle_t = \bar{n} - \sum_{n_-=0}^{\infty} \sum_{n_+=0}^{\infty} p(n_-) p(n_+) \sin^2 gt \sqrt{n}, \quad (3.271)$$

$$p(m) = \frac{\bar{n}^m}{m!} e^{-\bar{n}}, \quad (3.272)$$

$$\begin{aligned} \langle n^2 \rangle_t &= \bar{n} + \bar{n}^2 + \sum_{n_-=0}^{\infty} \sum_{n_+=0}^{\infty} p(n_-) p(n_+) \sin^2 gt \sqrt{n} \\ &\quad - 2\bar{n} \sum_{n_-=0}^{\infty} \sum_{n_+=0}^{\infty} p(n_-) p(n_+) \sin^2 gt \sqrt{n+1}. \end{aligned} \quad (3.273)$$

The time-averaged Mandel's factor is always positive here, which shows the super-Poisson number distribution for the total field. Since $\langle C_R \rangle_t$ and $V_t(C_R)$ can be transformed into $\langle S_R \rangle_t$ and $V_t(S_R)$, respectively, by the change $\delta_{+-} \rightarrow \delta_{+-} + k\pi/2$, it is enough to examine only one pair of these functions. In Fig.3.5, the Rabi oscillations of $V_t(C_R)$ are shown dependent on δ_{+-} at $\psi = 0$. At small δ_{+-} , the collapses and revivals behave quite typically for JCM, while the increase of δ_{+-} leads to a confluence of the nearest revivals. The Rabi oscillations of $\langle C_R \rangle_t$ have similar behavior. It should be emphasized that, unlike the previous case of single-atom radiation when the atomic phase induces the phase of the field, here the field phase defined through the complex amplitudes α_{\pm} induces the atomic phase (via the complex atomic amplitudes in the eq. (10)). This again clearly demonstrates the one-to-one correspondence between atomic and field phases.

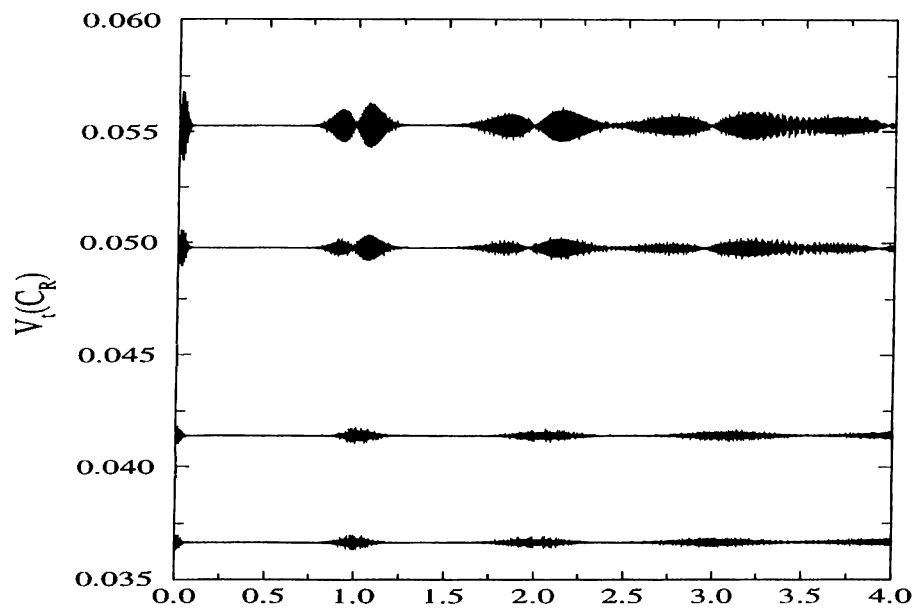


Figure 3.5: Evolution of the variance of the field cosine operator as a function of scaled time $t_s = gt/(2\pi(\bar{n}_- + \bar{n}_+)^{1/2})$ for $\bar{n}_\pm = 25$ and $g = 1$. Graphs from up to down correspond to the relative phases $\delta = 0, 45, 75, 90$ in degrees, respectively.

Chapter 4

Conclusion

General problem of light interacting with matter is studied by important and contemporary examples in the modern optical research. We have first examined the problem of generation and detection of squeezed phonons. We have presented a model for the effect of the longitudinal optical phonon number distribution on the Rabi oscillations of the photons involved in the associated indirect transition in a semiconductor heterostructure. It has been shown that a faster cavity photon revival rate occurs when phonons are initially in squeezed thermal state. This is the result of pairwise correlations of phonons in squeezed state and holds true when phonons are in squeezed vacuum or in squeezed number states. We have discussed the realization of this effect together with the possible generation scheme for such phonon states.

Besides, we have presented a more general scheme for detecting and classifying different non-classical states of Bose type excitations in solids. The methodology is based upon the relation between the photon correlations and correlations of scatterers in the three body scattering problem, like Raman scattering. Raman correlation spectroscopy combined with the ultrafast optical technology is shown to be valuable tool to demonstrate proposed scheme.

We have also worked on the problem of polarization of light at any distance. Development of the new approach in Ref.²⁶ for quantum phase has been performed for polarization and phase problems. According to that proposal, the process of

light generation should be taken into account to extend the operational approach. The cosine and sine operators were constructed by a polar decomposition of the angular momentum of radiative transition with the aid of conservation of angular momentum. We have confirmed that in the Jaynes-Cummings model the phase information is coherently transmitted from atom to radiation and vice versa. We have established connections of the cosine and sine operators to a set of generalized Stokes operators which are generalizations of the conventional Stokes operators with the inclusion of linearly polarized mode of radiation. Comparisons with the Pegg-Barnett phase formalism have revealed fundamental and qualitative differences in the quantum domain. A new effect called as phase bunching appeared in our case as a result of increased fluctuations due to the contributions from vacuum fluctuations of the linearly polarized mode.

Bibliography

- [1] E. S. Polzik, J. Carri and H. J. Kimble, *Phys. Rev. Lett.* **68**, 3020 (1992).
- [2] Ö.E. Müstecaplıođlu, Rabi oscillations in an exciton-polariton system, Master Thesis, Bilkent University, 1995.
- [3] A. S. Shumovsky and Ö.E. Müstecaplıođlu, *Phys. Lett. A* **209**, 88 (1995).
- [4] X. Hu and F. Nori, *Phys. Rev. B* **53**, 2419 (1996).
- [5] F. Nori, R. Merlin, S. Haas, A. W. Sandvik, and E. Dagotto, *Phys. Rev. Lett.* **75**, 553 (1995).
- [6] T. Hakiogđlu, V. A. Ivanov, A. S. Shumovsky, and B. Tanatar, *Phys. Rev. B* **51**, 15363 (1994).
- [7] J. Janszky, P. Adam, A. V. Vinogradov, and T. Kobayashi, *Spectrochim. Act.* **48A**, 31 (1992).
- [8] X. Hu, and F. Nori, *Phys. Rev. Lett.* **76**, 2294 (1996).
- [9] G. A. Garrett, A. G. Rojo, A. K. Sood, J. F. Whitaker, and R. Merlin, *Science* **275**, 1638 (1997).
- [10] M. Artoni, and J. L. Birman, *Phys. Rev. B* **44**, 3736 (1994).
- [11] S. E. Hebboul, and J. Wolfe, *Z. Phys. B* **73**, 437 (1989).
- [12] Ö.E. Müstecaplıođlu, and A. S. Shumovsky, *Appl. Phys. Lett.* **70**, 3489 (1997).

- [13] Ö.E. Müstecaplıoğlu, and A. S. Shumovsky, to be appear in *Phys. Rev.B* **60**, 1, 1999.
- [14] S. Gou, *Phys. Rev. A* **40**, 5116 (1989).
- [15] M. S. Kim, F. A. M. de Oliveira, and P. L. Knight, *Phys. Rev. A* **40**, 2494 (1989).
- [16] P. W. M. Blom, C. Smith, J. E. M. Havenkort, and J. H. Wolter, *App. Phys. Lett.* **62**, 2393 (1993).
- [17] P. A. M. Dirac, *Proc. R. Soc. London A* **114**, 243 (1927).
- [18] W. H. Louisell *Phys. Lett.* **7**, 60 (1963).
- [19] L. Suskind and J. Glogower, *Physics* **1**, 49 (1964).
- [20] P. Carruthers and N. Nieto, *Rev. Mod. Phys.* **40** (1968).
- [21] J. C. Garrison and J. Wong, *J. Math. Phys.* **11**, 2242 (1970).
- [22] D. T. Pegg and S. M. Barnett, *Europhys. Lett.* **6**, 483 (1988).
- [23] R. Tanaś, A. Miranowicz, Ts. Gantsong, in: *Progress in Optics*, Vol. 35, ed. E. Wolf (North-Holland, Amsterdam 1996).
- [24] J. W. Noh, A. Fougères and L. M'eres and L. Mandel, *Phys. Rev. Lett.* **67**, 1426 (1991).
- [25] A. Luis and L. L. Sánchez-Soto, *Phys. Rev. A* **48**, 4702 (1993c); Luis A., Sánchez-Soto L.L., and Tanaś R., *Phys. Rev. A* **51**, 1634 (1995).
- [26] A. S. Shumovsky, *Optics Comm.* **136**, 219 (1997),
- [27] A. S. Shumovsky and Ö.E. Müstecaplıoğlu, *Phys. Lett. A* **235**, 438 (1997).
- [28] V. I. Rupasov and M. Singh, *Phys. Rev. A* **54**, 3614 (1996).

- [29] M. Born and E. Wolf, *Principles of Optics* (Pergamon Press, New York), 1970.
- [30] J. M. Jauch and F. Rohrlich, *The Theory of Photons and Electrons* (Addison-Wesley, Reading), 1959.
- [31] J. D. Jackson, *Classical Electrodynamics*, (Wiley, New York), 1975.
- [32] W. Heitler, *The Quantum Theory of Radiation*, (3rd ed., Dover, New York), 1984.
- [33] A. S. Shumovsky and Ö.E. Müstecaplıođlu, *Jour. Mod. Opt.* **45**, 619, (1998).
- [34] A. S. Shumovsky and Ö.E. Müstecaplıođlu, *Phys. Rev. Lett.* **80**, 1202 (1998).
- [35] A. S. Shumovsky and Ö.E. Müstecaplıođlu, *Optics Comm.* **146**, 124 (1998)
- [36] H. T. Huang, and H. Zheng, *Solid State Commun.* **88**, 601 (1993).
- [37] H-I. Yoo, J. Sanchez-Mondragon, and J. H. Eberly, *J. Phys. A* **14**, 1383 (1981).
- [38] P. W. M. Blom, C. Smith, J. E. M. Havenkort, and J. H. Wolter, *App. Phys. Lett.* **62**, 2393 (1993).
- [39] D. Stoler, *Phys. Rev. D* **1**, 3217 (1970); **4**, 1925 (1971);
- [40] N.N. Bogolubov, *J. Phys. USSR* **11**, 23 (1947);
- [41] D. Robinson, *Comm. Math. Phys.* **1**, 159 (1965);
- [42] A. S. Shumovsky, in *Quantum Optics and the Spectroscopy of Solids*, edited by T. Hakioglu and A.S. Shumovsky (Kluwer, Dordrecht, 1997).
- [43] A.V. Chizhov, R.G. Nazmitdinov, and A.S. Shumovsky, *Quantum Optics* **3**, 1 (1991); *Mod. Phys. Lett. B* **7**, 1233 (1993).
- [44] T. Altanhan and B.S. Kandemir, *J. Phys.: Condens. Matter* **5**, 6729 (1993).

- [45] O. Madelung, *Introduction to Solid-State Theory* (Springer, New York, 1978).
- [46] L. Mandel and E. Wolf, *Optical Coherence and Quantum Optics* (Cambridge Univ. Press, Cambridge, 1994).
- [47] H. Haug and S. W. Koch, *Quantum Theory of the Optical and Electronic Properties of Semiconductors*, (World Scientific, Hong Kong, 1992).
- [48] A. Shumovsky and B. Tanatar, Phys. Rev. A **48**, 4735 (1993); Physics Lett. A **182**, 411 (1993).
- [49] L. Allen and J.H. Eberly, *Optical Resonance and Two-Level Atoms* (Dover, New York, 1987).
- [50] Y. R. Shen, *The Principles of Non-Linear Optics* (Wiley, NY, 1984).
- [51] D.F. Walls, J. Phys. A **6**, 496 (1973).
- [52] J. Peřina, Opt. Acta **28**, 325; 1529 (1981).
- [53] S. Carusotto, Phys. Rev. A **40**, 1848 (1989).
- [54] D.F. Walls, Z. Phys. **237**, 224 (1970).
- [55] R. Loudon, *The Quantum Theory of Light* (Oxford University Press, Oxford, 1983).
- [56] D. Chowdhury, *Spin Glasses and Other Frustrated Systems* (Princeton University Press, Princeton, NJ, 1986).
- [57] C. K. Law, L. Wang, and J. H. Eberly, Phys. Rev. A, **45**, 5089 (1992).
- [58] J. Peřina, *Quantum Statistics of Linear and Nonlinear Optical Phenomena* (D. Reidel Pub. Co., Dordrecht, 1984).
- [59] J.-C. Dier and W. Rudolph, *Ultrafast Laser Pulse Phenomena* (Academic Press, San Diego, 1996).

- [60] J. Shah, *Ultrafast Spectroscopy of Semiconductors and Semiconductor Nanostructures* (Springer, Berlin, 1996).
- [61] G. Arfken, "Mathematical Methods for Physicist", Academic Press, NY, (1970), 3rd.Ed., p.707.
- [62] E. H. Hill, "Theory of Vector Spherical Harmonics", Am. J. Phys. **22**, 211, (1954).
- [63] P. M. Morse and H. Feschbach, "Methods of Theoretical Physics", McGraw-Hill, NY, (1953)
- [64] J. M. Blatt and V. F. Weisskopf, "Theoretical Nuclear Physics", Wiley, NY, (1952).
- [65] J. Matthews, "Gravitational Multipole Radiation", in H. P. Robertson, In Memoriam. Philadelphia: Society for Industrial and Applied Mathematics (1963).
- [66] Davydov, Quantum Mechanics
- [67] C. J. Bouwkamp and H. B. G. Casimir, Physica **20**, 539, (1954)
- [68] Special issue on: Quantum Phase and Phase Dependent Measurements, Phys. Scripta T 48 (1993).
- [69] Ts. Gantsog and R. Tanaś, J. Mod. Optics **38** (1991) 1537.
- [70] V.I. Rupasov and V.I. Yudson, Sov. Phys. JETP **60** (1984) 927.
- [71] A. Vourdas, Phys. Rev. A **41** (1990) 1653.
- [72] H.S.M. Coxeter and W.O.J. Moser, Generators and Relations for Discrete Groups (Springer-Verlag, Berlin, 1965).